Title

Inhibition of the rebound burst of neural progenitor cells reduces ethanol seeking in female dependent rats: Regulation by neuroimmune and endothelial changes

Author

Nonoguchi, Hannah Aya

Publication Date

2022

Peer reviewed|Thesis/dissertation

UNIVERSITY OF CALIFORNIA SAN DIEGO

Inhibition of the rebound burst of neural progenitor cells reduces ethanol seeking in female dependent rats: Regulation by neuroimmune and endothelial changes

A Thesis submitted in partial satisfaction of the requirements
for the degree Master of Science

in

Biology

by

Hannah Aya Nonoguchi

Committee in charge:

Chitra Mandyam, Chair
Matthew Daugherty, Co-Chair
James Cooke
Brooke Pickett

2022

The Thesis of Hannah Aya Nonoguchi is approved, and it is acceptable in quality and form for publication on microfilm and electronically.

University of California San Diego

2022

DEDICATION

I dedicate this thesis to my family and friends who have always supported and believed in me. Thank you for your unconditional love.

EPIGRAPH

“I am among those who think that science has great beauty.”

Marie Curie

TABLE OF CONTENTS

LIST OF FIGURES

ACKNOWLEDGEMENTS

I would like to thank Dr. Chitra Mandyam for her support and guidance throughout my time as a master's student. Her knowledge and passion for research has shown me the power innovation and teaching have on the science community and the individual. I have found a love for research through her and cannot thank her enough for this life changing experience.

I would also like to thank my committee members Dr. Matthew Daugherty, Dr. James Cooke and Dr. Brooke Pickett for their guidance and encouragement to me and my project.

In addition, funds from the Department of Veterans Affairs (BX003304 to CDM), National Institute on Drug Abuse and National Institute on Alcoholism and Alcohol Abuse (AA020098) supported the study.

ABSTRACT OF THE THESIS

Inhibition of the rebound burst of neural progenitor cells reduces ethanol seeking in female dependent rats: Regulation by neuroimmune and endothelial changes

by

Hannah Aya Nonoguchi

Master of Science in Biology

University of California San Diego, 2022

Professor Chitra Mandyam, Chair
Professor Matthew Daugherty, Co-Chair

Alcohol use disorder (AUD) is highly prevalent in the United States with very few FDA approved treatments that do not completely reduce relapse to alcohol seeking. This is due to an incomplete understanding of the neurobiological substrates causing alcohol relapse. Previous studies in alcohol dependent male rats have shown cellular changes in the medial prefrontal cortex (mPFC), including increased oligodendrogenesis, heightened neuroimmune response, and decrease in blood-brain barrier (BBB) integrity associated with dependence induced drinking and relapse. Specifically during acute withdrawal, a proliferative burst of oligodendrocyte progenitor cells (OPCs) is prevalent in the mPFC which survive and mature

into oligodendrocytes. Research focused on male rats have shown this dysfunctional production of OPCs is linked to a heightened neuroimmune response and endothelial disruption, but unclear if these changes are evident in females as well. Thus, it was investigated if these non-neuronal changes were also evident in dependent female rats. Like in males, quantitative immunohistochemistry depicted an increase in Ki-67 cells in the mPFC of females during acute withdrawal and concomitant increase in Olig2 cells during protracted abstinence. In addition, 3D structural analysis, Western blotting and ELISA detected a heightened neuroinflammatory response after relapse, with an increase in microglia soma area and cytokines levels including NF-kB, TNF-α, IL-13, and IL-10 in the mPFC. Furthermore, ELISA data showed an increase in VEGF levels indicating BBB dysfunction. The next question investigated was whether preventing this burst of OPCs in dependent female rats will decrease ethanol seeking behavior by regulating the neuroimmune responses and endothelial changes. To prevent the generation of Ki-67 cells, a pharmacogenetic approach was used, where transgenic GFAP-TK rats were orally fed a DNA synthesis inhibitor called Valcyte during maintenance through reinstatement. Valcyte treatment decreased ethanol seeking behavior during relapse and reinstatement, as well as enhanced latency to extinguish ethanol behaviors, showing decreased motivation to alcohol drinking. In addition, Valcyte prevented microglia activation in the mPFC and normalized levels of TNF-α, IL-4, and IL-6 in the plasma. However, Valcyte did not prevent endothelial damage in the mPFC, indicated by an increase in Ve-Cadherin and decrease in Claudin-5 expression. In conclusion, preventing the proliferative burst of Ki-67 cells in the mPFC during acute withdrawal decreased ethanol seeking behavior and prevented some aspects of the immune response seen during relapse and reinstatement of ethanol seeking behaviors.

INTRODUCTION

Alcohol use disorder (AUD) affects approximately 20 million people in the United States (Mandyam *et al.*, 2017) and is associated with neurological deficits including decreased brain volume and cognitive impairment (Somkuwar *et al.*, 2016b). AUD is a type of addiction that has a systemic effect by negatively impacting multiple components of the body and can lead to cardiovascular and gastrointestinal disease, diabetes, cancer, and psychiatric disorders (Kranzler & Soyka, 2018). The pathology behind these diseases associated with AUD is linked to the production of reactive oxygen species (ROS) that result from the breakdown of alcohol to acetaldehyde leading to oxidative DNA damage (Fowler *et al.*, 2014). This oxidative damage leads to neuronal apoptosis causing impairments in learning, memory, and decision making (Mandyam *et al.*, 2017). Many individuals with moderate to severe AUD do not receive treatment and if they do, treatment is effective in only 30% of individuals. The ineffective treatments have led to only 20-50% of AUD individuals succeeding at short-term remission and within that small percentage about 80% will fail to maintain abstinence, ultimately leading to relapse (Somkuwar *et al.*, 2021). The lack of neurobiological understanding causing individuals with moderate to severe AUD to relapse has led to insufficient long-term treatments leaving the individual unable to combat this lifelong disorder. Thus, more studies on the neurobiological pathways that play a role in relapse are needed to make effective treatments for AUD.

When studying addiction, like AUD, Koob and Volkow (2010) addressed the three stages of addiction mediated by distinct neurocircuitry and brain regions. The three stages of addiction include: 1) binge and intoxication, 2) withdrawal and negative affect, 3) preoccupation and anticipation. The third stage, preoccupation and anticipation or the craving stage, is where individuals experience drug seeking behavior and the prefrontal cortex (PFC) plays a significant

role in this behavioral response. The PFC plays an important role in decision making and motivational instincts including reward and alcohol seeking (Somkuwar *et al.*, 2016a). These motivational instincts ultimately lead alcohol dependent individuals to relapse making alcohol addiction a chronic relapsing disorder. Thus, the PFC is an important brain region to study to understand what neuronal changes are happening during the craving stage and how to stop this addictive cycle.

To study the effects of alcohol on specific brain areas like the PFC, rodents including rats, are exposed to an experimental condition called chronic intermittent ethanol vapor exposure (CIE). CIE has successfully modeled moderate to severe AUD in rats by showing clinical signs of alcohol dependence including withdrawal symptoms and escalated ethanol drinking (O'Dell *et al.*, 2004). Additionally, CIE treated rats exhibited behaviors similar to alcohol dependent humans including anxiety-like behavior and determination to acquire alcohol (Avegno & Gilpin, 2019). By using the CIE rat model, we can study the behavior and neurobiology of alcohol dependent rats. In addition to modeling AUD, rodents have brain regions that are analogous to the human brains including the medial prefrontal cortex (mPFC), which is the functional and neuroanatomical homologue to human medial and dorsolateral PFC (Somkuwar *et al.*, 2016a). Hence, rats are an ideal mammalian model to study AUDs effects on specific brain regions.

Rodents are not only mammalian models for their homologous brain regions to humans, but also mimic the differences in drinking behavior seen between females and males. In humans, women are more vulnerable to ethanol abuse because of faster intoxication rates and become alcohol dependent faster than men (Randall *et al.*, 2017; Torres *et al.*, 2014). In rodents, females voluntarily drink more ethanol than males through greater lever pressing, meaning females experience greater rewarding effects from ethanol (Torres *et al.*, 2014). In addition, the same

study showed the female hormone cycle contributed to the difference in susceptibility to the rewarding effect of alcohol. When ovaries are taken out of female rats, no enhanced rewarding effects of ethanol are prominent, suggesting that ovarian hormones influenced the reward system distinctly in females (Torres *et al.*, 2014). Interestingly, female rats show less motivational withdrawal to alcohol during reinstatement than males (Becker & Koob, 2016). These studies show a distinct sex differentiation in alcohol dependency. Thus, we must understand the differences that arise neurobiologically between AUD males and females in order to have better, more specific treatments for both genders.

Previous research has shown chronic alcohol exposure not only affects neurogenesis, but non-neuronal factors in the brain of alcohol dependent male rats as well. This includes changes in blood-brain barrier (BBB) integrity, neuroinflammation, and gliogenesis (Somkuwar *et al.*, 2017a). In alcohol dependent male rats, there is a decrease in BBB integrity, an increase in neuroinflammation and the production of malfunctioning oligodendrocytes that negatively impacts cognitive ability. Detrimental non-neuronal changes due to chronic alcohol exposure should be the basis for future studies because of their long-lasting effects on structural brain integrity and homeostatic conditions that contribute to impaired cognitive function.

Chronic alcohol exposure has been shown to disrupt the BBB that consists of endothelial cells that separate the brain from other molecules, proteins, and foreign substances to keep a homeostatic environment. A key component of endothelial cells in the BBB is platelet endothelial cell adhesion molecule-1 (PECAM-1). PECAM-1 is a cell junctional protein found in vascular cells that help with BBB integrity and permeability of different components that control inflammation especially in response to oxidative stress (Mandyam *et al.*, 2017). PECAM-1 is also angiogenic by forming new blood vessels that support the production of OPCs. In alcohol

dependent rats, ethanol gets metabolized to produce ROS leading to elevated PECAM-1 levels which is associated with a decrease in BBB integrity, hyperoligodendrogenesis, and increased alcohol seeking (Mandyam *et al.*, 2017). During chronic alcohol exposure, a leaky BBB and enhanced PECAM-1 expressions allow outside factors including cytokines and leukocytes inside the brain. This influx of immune factors leads to a chronic inflammatory response including activating NF-kB signaling and microglia causing neuronal damage (Mandyam *et al.*, 2017). A crucial next step is knowing if preventing BBB damage and decreasing PECAM-1 levels in CIE rats can prevent the increase in inflammatory response, oligodendrogenesis, and alcohol seeking.

Recent findings from Dr. Mandyam's laboratory suggest that preventing BBB damage and blocking PECAM-1 expression via Endostatin, can cause a decrease in oligodendrogenesis in the mPFC and ethanol seeking behavior (Avchalumov *et al.*, 2021). Endostatin is an angiogenesis inhibitor that stops the proliferation of endothelial cells reversing elevated expression of PECAM-1 and preventing production of OPCs. Interestingly in Avchalumov *et al.* (2021), the CIE female rats treated with Endostatin had reduced relapse to drinking behavior associated with decreased survival of oligodendrocytes and microglia activation. In contrast, blocking PECAM-1 expression using Endostatin in CIE male rats did not affect or relapse to drinking, oligodendrogenesis production, or activation of microglia (Avchalumov *et al*., 2021). In alcohol dependent female and male rats, sex-specific responses are evident through differences in how PECAM-1 affects neurological mechanisms and behavior during abstinence. This research brought to light a huge endeavor that must be explored; despite the importance of understanding how AUD affects sexes differently, few studies have focused on comparing

neuroplasticity and behavior between males and females especially during withdrawal and protracted abstinence.

In addition to a decrease in BBB integrity and increase in PECAM-1 expression, AUD upregulates neuroinflammatory pathways linked to increased NF-kB signaling and microglia activation allowing the release of cytokines inducing a chronic inflammatory response in the brain (Mandyam *et al.,* 2017; Siemsen *et al.*, 2021). In addition, gene expression profiling has depicted an upregulation of IL-3 and TNF signaling pathway in mPFC of male rodents (Warden *et al.,* 2020). An aspect of focus to indicate changes in neuroimmune response is differences in microglia morphology when in the resting or activated state. Microglia in a resting state have a smaller soma volume, thin elongated processes, and ramified complex branching leading to more intersections per distance from soma (Siemsen *et al*., 2021; Wang *et al*., 2018). While activated microglia, also referred to as in the ameboid state, is characterized by an enlarged soma, thicker retracted processes, and a decrease in the number of intersections per distance from soma meaning less branching complexity. Previous studies have shown that during acute withdrawal, the microglia somatic volume of male CIE rats is subtly increased in the mPFC indicating an increase in a neuroimmune response (Siemsen *et al.*, 2021) that can potentially be detrimental to cognitive function including learning and memory. Activation of microglia and neuroimmune factors play an important role in behavior, but few research studies look at specific neuroimmune factors in the mPFC of CIE female rats during protracted abstinence. Thus, we aim to examine neuroimmune expression in alcohol dependent female rats and its effect on behavior.

In addition to decreased BBB integrity and heightened immune response, CIE has been shown to cause a change in oligodendrogenesis associated with increased ethanol seeking in alcohol dependent male rats (Somkuwar *et al.*, 2017a). Oligodendrocytes are a type of glia cell

that myelinate neurons to aid in neuronal signaling and originate from oligodendrocyte progenitor cells (OPCs). When studying the mPFC of male rats during CIE maintenance there was a suppression of OPC proliferation. But in acute withdrawal, a rebound effect involving a proliferative burst of OPCs is produced that has been correlated with heightened anxiety and stress (Somkuwar *et al.*, 2016b; Somkuwar *et al.*, 2017b). The hyperproliferative OPCs survive and mature into myelinating oligodendrocytes in protracted abstinence causing maladaptive plasticity and higher propensity for relapse (Somkuwar *et al.*, 2016 a,b). These studies suggest enhanced oligodendrogenesis during acute withdrawal is a compensatory mechanism to recover the gliogenesis loss during CIE maintenance (Mandyam *et al.*, 2017). This compensatory mechanism leading to maladaptive plasticity is depicted by an increase in flayed myelin linked to a decline in cognitive performance due to reduced ability to recall memories (Somkuwar *et al.*, 2021). Therefore, research should focus on how blocking this compensatory mechanism could stop impaired cognitive function and reduce alcohol seeking.

In this study, we want to understand if the burst of OPCs seen in acute abstinence causes long term effects including a heightened immune response, BBB damage, and increased alcohol seeking in the understudied female rats. To inhibit this proliferation of OPCs, we used a pharmacogenetic approach, where transgenic female rats expressing herpes simplex virus-thymidine kinase (HSV-TK) under the human GFAP promoter (GFAP-TK) were orally fed Valcyte during maintenance until the day of euthanasia (Fannon e*t al.*, 2018). The viral thymidine kinase phosphorylates Valcyte, allowing the drug molecule to be incorporated into the DNA strand blocking DNA polymerase activity, thus stopping cell division inducing apoptosis of newly born progenitor cells. Through the use of Valcyte treatment, we hypothesize that preventing the proliferative burst of neural progenitor cells during acute withdrawal in alcohol

dependent female rats will reduce ethanol seeking behavior by regulation of the neuroimmune response and endothelial changes. Previous studies have focused on alcohol dependent male rats, but not females. My research focuses solely on female rats to help elucidate the non-neuronal changes that chronic ethanol exposure causes in the mPFC into protracted abstinence. Specifically, if stopping the production and survival of maladaptive oligodendrocytes can directly change ethanol seeking behavior and neurobiological responses. This study will lead to a better understanding of how chronic alcohol exposure affects the neurobiological pathways in females over time to make more effective long-term treatments for both genders with alcohol use disorder.

METHODS AND MATERIALS

Animals

Transgenic rats expressing HSV-TK under the human GFAP promoter (GFAP-TK) were generated on a Long–Evans background (Snyder *et al.*, 2016). These rats were bred at the VA San Diego vivarium. Rats were weaned at 21–24 d of age, pair-housed, and genotyped in house by qPCR. The rats were housed two-three/cage in a temperature-controlled (22°C) vivarium on a 12 h/12 h light/dark cycle (lights on 8:00 P.M- 8:00 A.M.). All procedures were performed during the dark phase of the light/dark cycle. Food and water access was available *ad libitum*. All rats weighed approximately 180-250 g and were 8 weeks old at the beginning of the study. All experimental procedures were carried out in strict adherence to the National Institutes of Health Guide for the Care and Use of Laboratory Animals (NIH publication number 85–23, revised 1996) and approved by the Institutional Animal Care and Use Committee of VA San Diego Healthcare System.

Ethanol Self-Administration

The behavioral experiments conducted herein are presented as a detailed schematic in Figure 1. Thirty two transgenic female rats were given one to two 14-hour lever-responding training sessions in the operant conditioning boxes (Med Associates Inc, VT), on an fixed-ratio 1 schedule (FR1; one response resulted in one reinforce delivery), where one press on the available lever resulted in the delivery 0.1ml of water to a sipper cup mounted on the wall in between the two levers. The operant conditioning boxes were housed inside sound attenuating chambers. During these sessions, the house-light and white noise were turned off. Then, rats were trained to respond for 0.1ml of alcohol (10% v/v) over four daily 2-h FR1 sessions; all other conditions remained the same as before. Subsequently, the rats were trained to discriminate between two

available levers to obtain 0.1 ml ethanol (10% v/v) during daily 30-min FR1 sessions. During these sessions, active (right) lever responding resulted in the delivery of ethanol, while responding on the inactive (left) lever was recorded but had no programmed consequence. Each ethanol delivery followed by a 4-sec time-out during which responding on the active lever did not result in the delivery of ethanol. During this time-out period, the cue-light above the active lever remained on; thus the cue-light was paired with the delivery of ethanol. These 30-min discrimination training sessions continued till stable responding was obtained, where stable responding was defined as less than 10% variation in active lever responding for 3 consecutive 30-min FR1 sessions.

Subsequently, the rats received chronic intermittent ethanol vapor exposure (CIE; see procedure below) for a duration of 7 weeks. Henceforth, these rats will be called CIE-ED (alcohol dependent, n=32). All rats received two 30-min FR1 sessions per week (Tuesdays and Thursdays) during these 7 weeks. Responding was analyzed to determine escalation of self-administration compared to pre-vapor stable responding. After 7 weeks of CIE, CIE-ED rats were withdrawn from ethanol vapors and from ethanol self-administration. The CIE-ED rats were divided into two groups (vehicle or Valcyte; see below) and maintained as described for the remainder of the study.

Chronic intermittent ethanol vapor exposure (CIE)

During CIE, rat cages were housed in specialized chambers and were exposed to alcohol vapors on a 14-h ON / 10-h OFF schedule. Alcohol (95% ethanol) from a large reservoir was delivered to a heated flask at a regulated flow rate using a peristaltic pump (model QG-6, FMI Laboratory, Fluid Metering). The drops of alcohol in the flask were immediately vaporized and

carried to the vapor chambers containing the rat cages by controlled air flow (regulated by a pressure gauge). The air pressure and ethanol flow rates were optimized to obtain blood alcohol levels (BALs) between 125 and 250 mg/dl or 27.2 and 54.4 mM (Gilpin *et al.*, 2008); these BALs are 2-3 times the BAL observed in binge drinking, but not high enough to abolish righting reflex (Courtney & Polich, 2009; Ernst *et al.*, 1976).

Tail bleeding for determination of BAL

For measuring BALs, tail bleeding was performed on the CIE-ED rats, once a week (every Tuesday), between hours 13-14 of vapor exposure (Gilpin *et al.*, 2008). Rats were gently restrained while the tip of the tail was pricked with a clean needle. Tail blood (0.2 ml) was collected and centrifuged at 2000 rpm for 10 min. Plasma (5 μL) was used for measurement of blood alcohol levels (BALs) using an Analox AM1 analyzer (Analox Instruments USA Inc., MA). Single-point calibrations were performed for each set of samples with reagents provided by Analox Instruments (100 mg/dl). When plasma samples were outside the target range (125–250 mg/dl), vapor levels were adjusted accordingly.

Valcyte Treatment

Proliferation of progenitor cells was suppressed by feeding the animals the orally available prodrug, valganciclovir (Valcyte, Roche), which is enzymatically converted to ganciclovir. Valcyte (7.5 mg) was given in a 0.5 g pellet of a 1:1 mixture of ground chow and almond butter. To minimize neophobia, rats were exposed to the chow–almond butter mixture in their home cage for 2-4 days prior to drug treatment. On drug treatment days, each rat was separated into an empty cage without bedding and individual Valcyte pellets were placed on the wall of the cage and monitored for feeding activity to ensure consistent dosing. Once the animal

consumed the drug pellet the animal was moved back to the housing chamber. The entire feeding procedure lasted between 4-7 minutes and care was taken to reduce any stressful experience. Valcyte treatment (1x/d) was initiated during week 6 of CIE and was continued until the day of euthanasia. All CIE-ED animals consumed the vehicle or Valcyte chow/almond butter pellet (+/− Valcyte; females, n = 24 CIE vehicle, n = 9 Valcyte).

Drinking during abstinence, Relapse

After 3 weeks of abstinence from CIE and ethanol self-administration, CIE-ED rats, both with and without Valcyte, were given one 30 min FR1 session to lever press for ethanol reinforcement (0.1 ml of 10% v/v ethanol) under cue-context conditions identical to that used for training and maintenance. Active and inactive lever responses were recorded.

Extinction

Following relapse, rats were subject to 6 daily 30-min extinction sessions under a different cue-context combination than that used for training and maintenance. Specifically, operant boxes different from those used for self-administration were used and the house-light and white noise were turned on, and no cue-lights were available following lever presses. Finally, the lever response did not result in the delivery of ethanol. Both lever responses were recorded.

Reinstatement

Following the 6th day of extinction, rats were subject to one session of cued-context reinstatement of ethanol seeking. Specifically, rats were introduced to operant chambers under conditions identical to training and maintenance (no house-light, no white noise). Active lever

responses resulted in the presentation of the cue-light for 4 sec, but did not result in the delivery of ethanol. Both active and inactive lever responses were recorded.

Brain tissue collection

Rats were euthanized by rapid decapitation and the brains were isolated, and dissected along the midsagittal plane. The left hemisphere was snap frozen for Western blotting analysis and multiplex cytokine immunoassays and the right hemisphere was postfixed in 4% paraformaldehyde for immunohistochemistry. For tissue fixation, the hemispheres were incubated at room temperature for 36 hours and subsequently at 4°C for 48 hours with fresh paraformaldehyde replacing the old solution every 12 hours. Finally, the hemispheres were transferred to sucrose solution (30% sucrose with 0.1% sodium azide) for cryoprotection and storage till tissue sectioning was conducted (Cohen *et al.*, 2015). Subsequently, the tissue was sliced in 40µm sections along the coronal plane on a freezing microtome. Every ninth section through the PFC (+3.7 to +2.5 mm from bregma; 4 sections per rat) was mounted on Superfrost® Plus slides and dried overnight and used for Ki-67 analysis. Two sections through the PFC (+3.2 and +2.7 mm from bregma) were mounted as described before and processed for IBA-1 and Olig2 analysis. The sections were pretreated, blocked, and incubated with the primary antibody followed by biotin-tagged secondary antibody. Staining was visualized with 3,3′-diaminobenzidine chromogen (DAB; cat# SK-4100; Vector Laboratories, Burlingame, CA, USA).

Immunohistochemistry (IHC) and cell counting of Ki-67 and Olig2

For Ki-67 (rabbit polyclonal, 1:1000, catalog # RM-9106-S, Thermo Scientific) and Olig2 (generous gift from Dr. Charles Stiles, Harvard Medical School), quantitative

immunohistochemical assay was performed using a previously published optical fractionator method (Kim *et al.*, 2015) . Ki-67 labeled cells were quantified in the mPFC with a Zeiss AxioImager Microscope equipped with Stereo Investigator 16 (MicroBrightField Bioscience, Williston, VT USA), a three-axis Mac 5000 motorized stage, a Zeiss digital MRc video camera, PCI color frame grabber, and computer work station. mPFC regions were contoured by referencing histological landmarks including corpus callosum, anterior commissure and rhinal fissure, using a 5x objective with a 10x eyepiece and the above software (Paxinos and Watson, 1997). Cells were visually quantified within the contour using a 20x objective and a 10x eyepiece by an observer blind to the study using the following criteria - cells stained as dark brown to black, with the ability to focus the boundary of the cell within the mounted section thickness. A software generated 180 X 120 μm counting frame was systematically moved through the entire contoured area of the tissue to manually assess and count the Ki-67 positive (Ki-67+) cells. Mounted section thickness after immunohistochemistry was determined to be ~28 μm. The Ki-67+ cells always appeared in clusters of irregularly shaped dark stained cells. The overlapping-pair arrangement and the number of cells in each cluster were confirmed by focusing on different layers of cells along the Z-axis. Absolute cell counting (complete counting of all immunoreactive cells in the contoured area) was performed in the mPFC; the data are presented as total number of cells per unit area (cells/mm^2 based on mounted section thickness) per animal. Ki-67 cells were also counted in the subventricular zone and are reported as cells per mm2.

For Olig2 staining, the sections were pretreated (Mandyam *et al.*, 2004), blocked, and incubated with the primary antibody followed by biotin-tagged secondary antibody. Olig2 immunoreactive cells were examined and quantified with a Zeiss AxioImager Microscope as

described previously. Live video images were used to draw contours delineating the subregions of the PFC (anterior cingulate, prelimbic and infralimbic cortices). The fields of the brain regions for quantification were traced separately at 25x magnification. A 150 x 150 μm frame was placed over the regions of interest using the StereoInvestigator stereology platform followed by analysis using the optical fractionator method. The frame was systematically moved over the tissue to cover the entire contoured area and the labeled cells in each subregion falling entirely within the borders of the contour were marked and analyzed. Immunoreactive cells were quantified (absolute cell counting in the area contoured for analysis) and were summed up for each PFC subregion and summed up and reported as cells per mm^2.

Analysis of microglial cells in mPFC

Immunohistochemical assay of IBA-1 was performed on the mPFC using a previously published method. The mPFC was stained with rabbit anti IBA-1 (019-19741,1:1000; Wako) to view structural differences of microglial cells (Takashima *et al.*, 2018).

Zeiss AxioImager A2 microscope was used to view the structures and Neurolucida; Micro-BrightField (a computer-based program) was used to create three dimensional tracings that were analyzed by Neurolucida Explorer; Micro-BrightField (a computer-based program). The following criteria was used to access the efficacy of microglial cells: (1) the cell was in the mPFC (the region of interest), (2) the cell was specifically defined from other cells, (3) the cell was fully intact and not broken, (4) the cell was stained dark enough to visualize the soma and processes. 6 cells were traced for each animal, 3 traces for each of the two sections. 40x magnification with an oil immersion lens (equipped with a 10x eyepiece) was used to view and trace the cells. After tracing, soma area, soma to tip distance, total process length, and 3D Sholl

analysis was performed to see the total number of process intersections relative to the radial distance (starting from 0 mm and increasing in 1 mm in from the soma).

Western Blotting

Procedures optimized for measuring both phosphoproteins and total proteins were performed as previously described (Kim *et al.*, 2014; Galinato *et al.*, 2015; Navarro & Mandyam, 2015; Staples *et al*., 2015). Tissue was homogenized in a refrigerated bead mill homogenizer (Next Advance) in buffer (320 mM sucrose, 5 mM HEPES, 1 mM EGTA, 1 mM EDTA, 1% SDS, with Protease Inhibitor Cocktail and Phosphatase Inhibitor Cocktails II and III diluted 1:100; Sigma), heated at 95 degrees C for five minutes, and stored at -80 degrees C until determination of protein concentration by a detergent-compatible Lowry method (Bio-Rad, Hercules, CA). Samples were mixed (1:1) with a Laemmli sample buffer containing β-mercaptoethanol. Each sample containing protein from one animal was run (20 μg per lane) on 10% SDS-PAGE gels (Bio-Rad) and transferred to polyvinylidene fluoride membranes (PVDF pore size 0.2 μm). Blots were blocked with 5% milk (w/v) in TBS (25 mM Tris-HCl (pH 7.4), 150 mM NaCl) for one hour at room temperature and were incubated with the primary antibody for 16-20 h at 4 °C: antibody to Claudin-5 (mouse monoclonal, 1:500, Invitrogen, cat. no. 35-2500, predicted molecular weight 25 kDa, observed band ~20 kDa); Cox-2 (rabbit monoclonal, 1:200, Cell Signaling, cat. no. 12282S, molecular weight 74 kDa, observed band ~75 kDa); total NF-kBp65 (rabbit polyclonal, 1:500, Cell Signaling, cat. no. 8242S, molecular weight 65 kDa, observed band ~65 kDa); pNF-kBp65 at Ser536 (rabbit monoclonal, 1:200, Cell Signaling, cat. no. 3303L, molecular weight 65 kDa, observed band ~65 kDa); Ve-Cadherin (mouse monoclonal, 1:100, Santa Cruz Biotechnology, cat. no. sc-52751, molecular weight 130kDa, observed band ~60 kDa). Blots were then washed three times for 5 min in TBST, and then

incubated for 1 h at room temperature with horseradish peroxide–conjugated goat antibody to mouse or rabbit in 2.5% milk in TBS. Following subsequent washes, immunoreactivity was detected using SuperSignalWest Dura chemiluminescent detection reagent (Thermo Scientific, Waltham, MA, USA) and images were collected using a digital imaging system (Azure Imager c600, VWR, Radnor, PA, USA). For normalization purposes, membranes were incubated with 0.125% Coomassie stain for 1-2 min and washed three times for 5–10 min in destain solution (Welinder & Ekblad, 2011; Thacker *et al.*, 2016). Densitometry was performed using ImageJ software (NIH). The signal value of the band of interest following subtraction of the background calculation was then expressed as a ratio of the corresponding coomassie signal (following background subtraction). This ratio of expression for each band was then expressed as a percent of the adult female sedentary rat included on the same blot.

Multiplex cytokine immunoassays

Cytokine levels in plasma and brain tissue homogenates were analyzed using a custom Meso Scale Discovery rat cytokine v-plex panel, allowing for the measurement of interferons (IFN-g), interleukins (IL-1β, IL-4, IL-5, IL-6, IL-10, IL-13), chemokines (KC/GRO (CXCL1)), and adipokines (TNF-α; (catalog #: K15059D, MSD, Rockville, MD)), and VEGF r-plex, allowing for the measurement of rat VEGF-A (catalog #: F231F). Plasma samples were diluted by adding 30ul plasma to 90ul of diluent provided with the kit and 50ul of the diluted plasma was used per well. Brain protein extracts were normalized to 1ug/ul and diluted by adding 10ul of protein extract to 40ul of diluent per well. Plates were read with a Sector Imager 2400, and data analyzed using the MSD Discovery Workbench software v. 4.0 (MSD, Rockville, MD). The lower limit of detection (LLOD) for the assays varied by analyte. The following are LLOD for each marker (pg/mL): IFN-γ: 0.65, IL-1β: 6.92, IL-4: 0.69, IL-5: 14.1, IL-6: 13.8, IL-10: 16.4,

IL-13: 1.97, KC/GRO (CXCL1): 1.04, TNF-α: 0.72 and VEGF: 0.69. Values falling below the LLOD were replaced with 0 pg/mL in all analyses and figures. IL-5 was not detected in plasma.

Statistical analysis

Ethanol behavior was analyzed with two-way ANOVA or two-tailed paired t-test followed by post hoc analysis (Fisher's LSD). Immunohistochemical data was analyzed by two-way ANOVA or one-way ANOVA or two tailed unpaired t-test followed by post hoc analysis (Fisher's LSD). Western blotting data and Multiplex cytokine immunoassays were analyzed with one-way ANOVA or two-tailed unpaired t-test. GraphPad Prism was used for data analysis with significance set at $p \leq 0.05$.

FIGURES

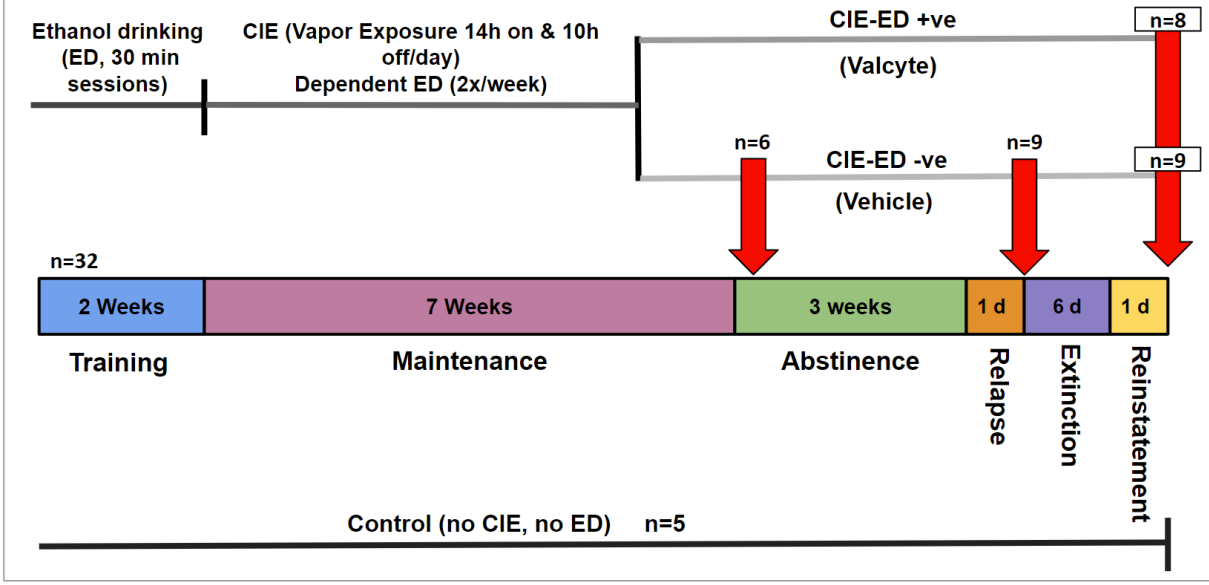

Figure 1: Schematic representation of experimental timeline
Female rats were trained to self-administer ethanol for 2 weeks. Then they went through 7 weeks of maintenance, involving exposure to ethanol vapors on a constant cycle daily and self-administered ethanol 2 times a week (CIE-ED). Starting at week 6 of maintenance, the rats were divided into two groups, with no Valcyte (-ve, vehicle) or Valcyte (+ve, Valcyte) treatment. The Valcyte (CIE-ED +ve) rats were orally fed Valcyte in a ground chow and almond butter pellet (n = 8). The pellet drug was given once a day the last week of maintenance and three times a week during abstinence until the day of euthanization after reinstatement. The vehicle (CIE-ED -ve) rats were not given any Valcyte, only almond butter throughout the experiment (n = 9). Both groups experienced 3 weeks of abstinence with no ethanol vapor exposure or self-administered ethanol. Following abstinence, rats went through a one 30 min FR1 session to lever press for ethanol reinforcement, followed by 6 daily 30-min extinction sessions under a different cue-context and one session of cue-context reinstatement of ethanol seeking. Some CIE-ED -ve rats were euthanized 3 days into abstinence (n = 6) and after relapse (n = 9). CIE-ED -ve (n = 9) and CIE-ED +ve (n = 8) rats were euthanized 45-2hr after reinstatement. The control group experienced no CIE or ED and were age matched (n = 5).

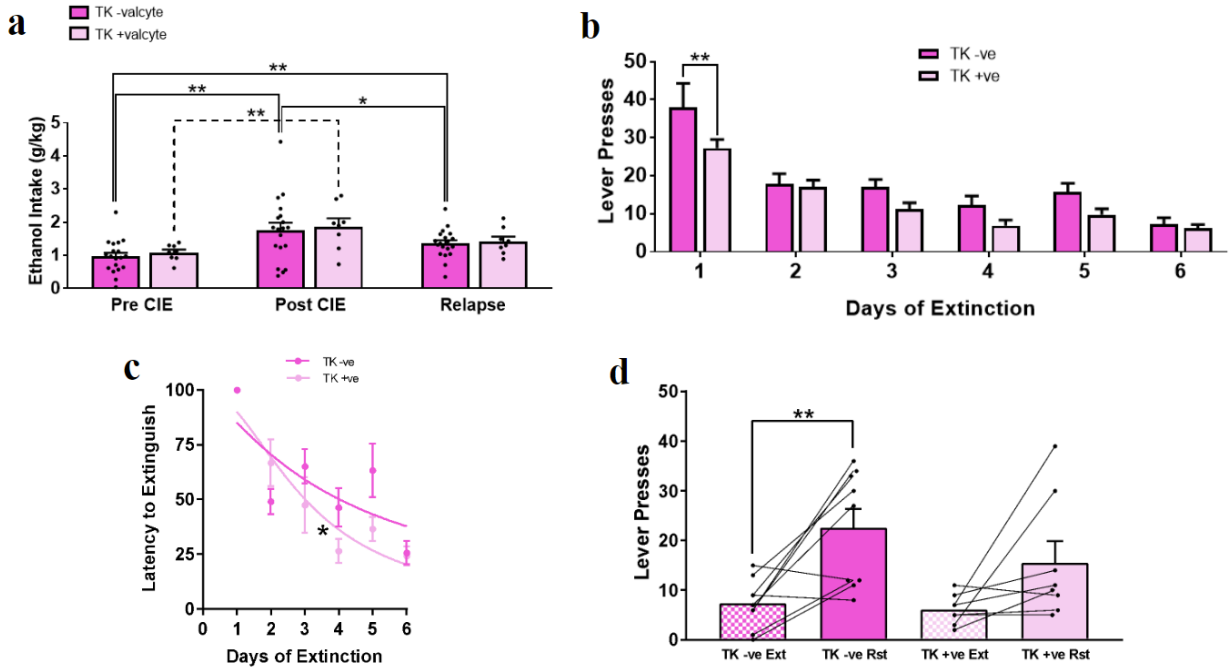

Figure 2: Behavioral responses in +Valcyte and -Valcyte rats during relapse, extinction (Ext), and reinstatement (Rst)

(a) Ethanol intake (g/kg) for -ve and +ve groups before CIE, post CIE maintenance, and after relapse. -ve: $^{**}p \leq 0.005$ between pre CIE and post CIE, $^{*}p \leq 0.05$ between post CIE and relapse, and $^{**}p \leq 0.005$ between pre CIE and relapse represented with the solid lines. +ve: $^{**}p \leq 0.005$ between pre CIE and post CIE represented with the dashed line. (b) Active lever responses during the 6 days of extinction in -ve and +ve groups, $^{**}p \leq 0.005$ between -ve and +ve groups day 1 of extinction. (a,b) Group differences were calculated by two-way ANOVA. (c) Nonlinear regression analysis for latency to extinguish by percent change from day 1 of extinction for -ve and +ve groups, $^{*}p \leq 0.05$. (d) Active lever responses during day 6 of extinction followed by reinstatement in -ve and +ve rats. Two-tailed paired t-test in -ve group revealed: $^{**}p \leq 0.005$ between Ext and Rst. Error bars represent standard error of the mean.

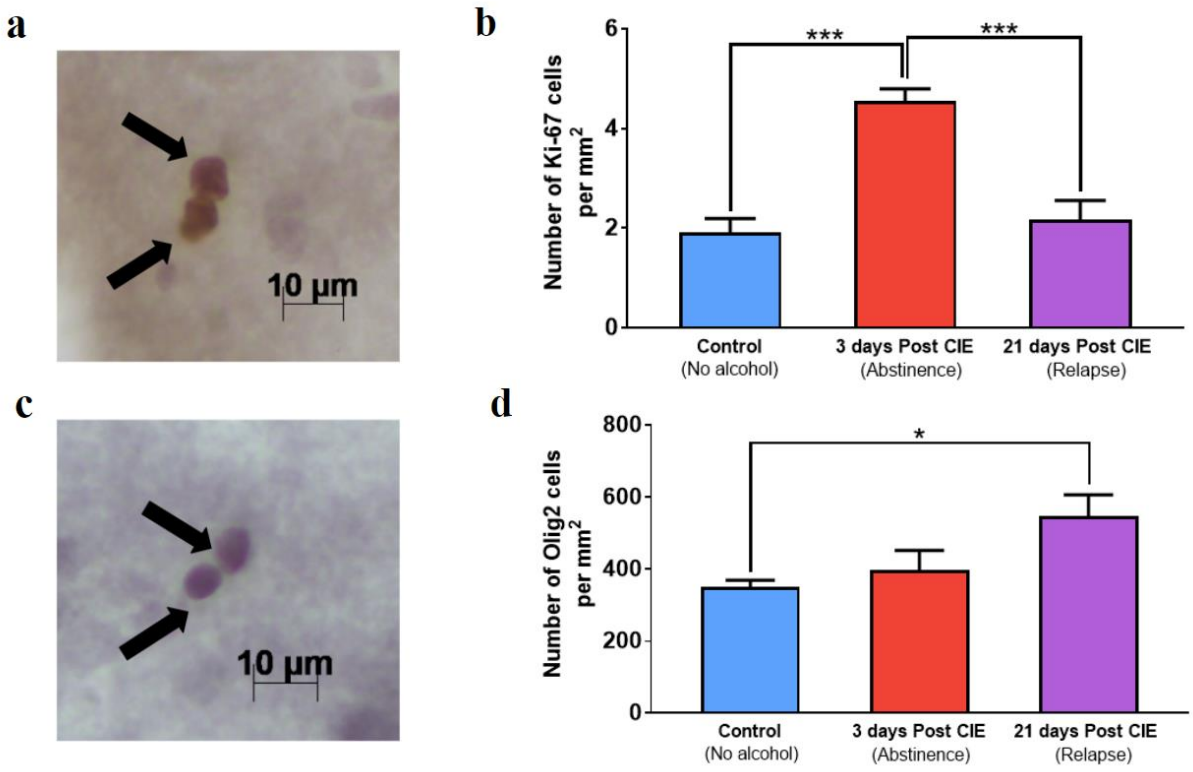

Figure 3: Ki-67 and Olig2 expression in the mPFC of alcohol dependent rats 3 days into abstinence and after relapse

(a) DAB stained Ki-67 cells in the mPFC with an arrowhead pointing to immunolabeled cells. (b) Number of cells expressing Ki-67 in the mPFC of rats, normalized to cells/mm^2 during different timepoints. Significant group differences were calculated using one-way ANOVA and post hoc analysis: ***$p \leq 0.0005$ between control and 3 days post CIE; ***$p \leq 0.0005$ between 3 days post CIE and 21 days post CIE. (c) DAB stained Olig2 cells in the mPFC with an arrowhead pointing to immunolabeled cells. (d) Number of cells expressing Olig2 in the mPFC of rats, normalized to cells/mm^2 during different timepoints. Significant group differences were calculated using one-way ANOVA and post hoc analysis: *$p \leq 0.05$ between control and 21 days post CIE. Error bars represent standard error of the mean.

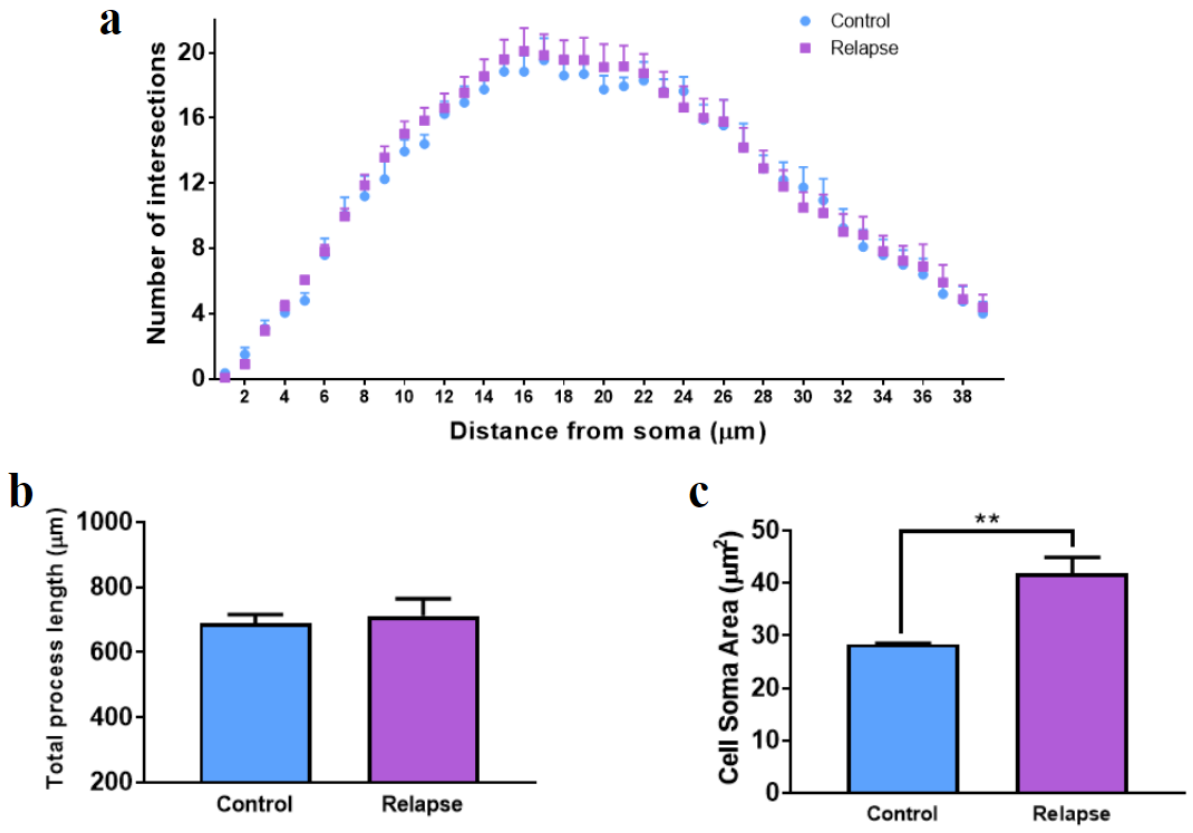

Figure 4: Phenotypic analysis of microglia (IBA-1 cells) in the mPFC of alcohol dependent rats after relapse The mPFC was stained for IBA-1, a marker for microglia. IBA-1 stained microglia were traced using Neurolucida and quantified using Neurolucida Explorer. (a) Structural analysis of mPFC microglial cell process is shown as the number of intersections relative to the distance from soma in micrometers. Two-way ANOVA with multiple comparisons revealed no significant difference between control and relapse group, $p \leq 0.05$. Two-tailed unpaired t-test revealed: (b) No significant difference in total process length between control and relapse, $p \leq 0.05$. (c) Significant difference in cell soma area: $^{**}p \leq 0.005$ between relapse and control. Error bars represent standard error of the mean.

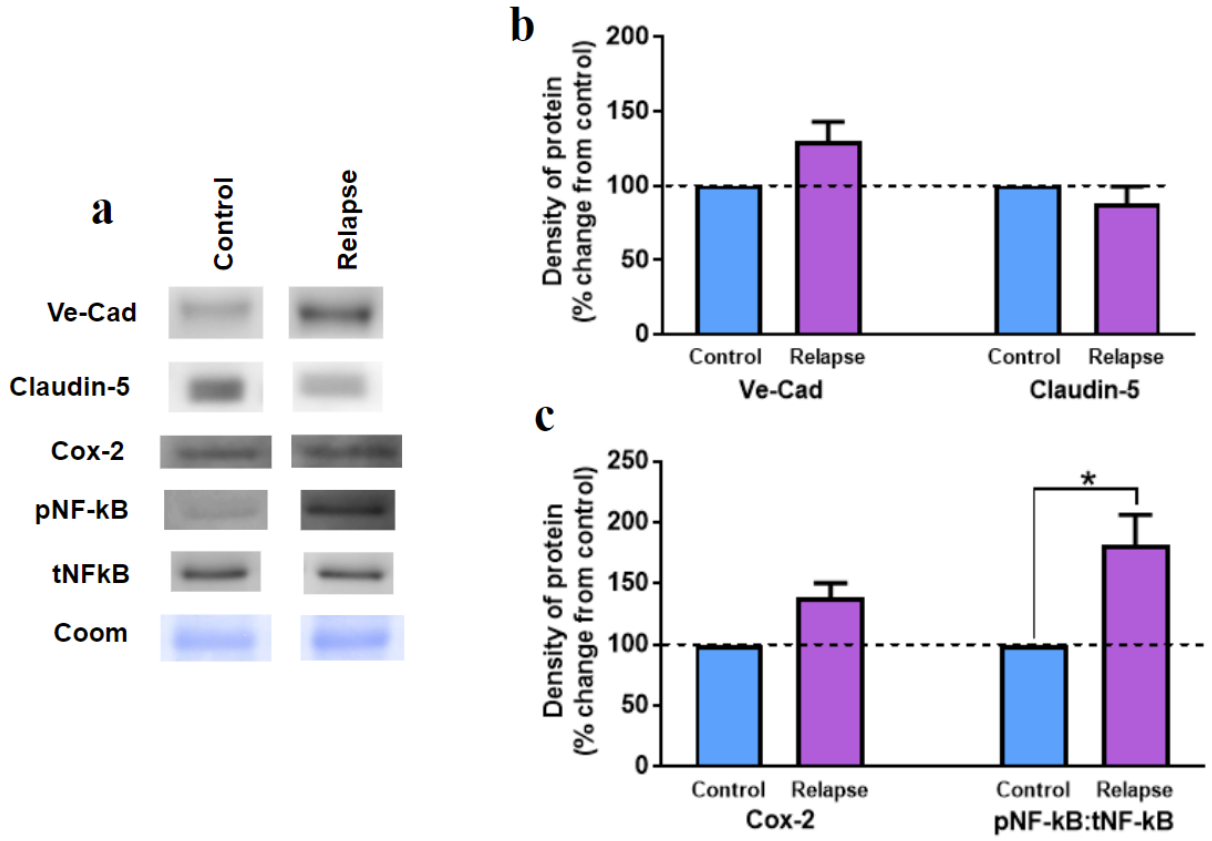

Figure 5: Western blot analysis of endothelial and neuroimmune markers in the mPFC of alcohol dependent rats after relapse

Representative immunoblots with corresponding Coomassie (Coom) blot is indicated in (a) Ve-Cadherin (Ve-Cad), Claudin-5, Cox-2, phospo NF-kB (pNF-kB), and total NF-kB (tNF-kB). (b,c) Quantitative data represented as mean ± S.E.M of percent change in density of protein from respective controls (indicated as a dashed line). (c) *$p \leq 0.05$ between control and relapse in pNF-kB:tNF-kB.

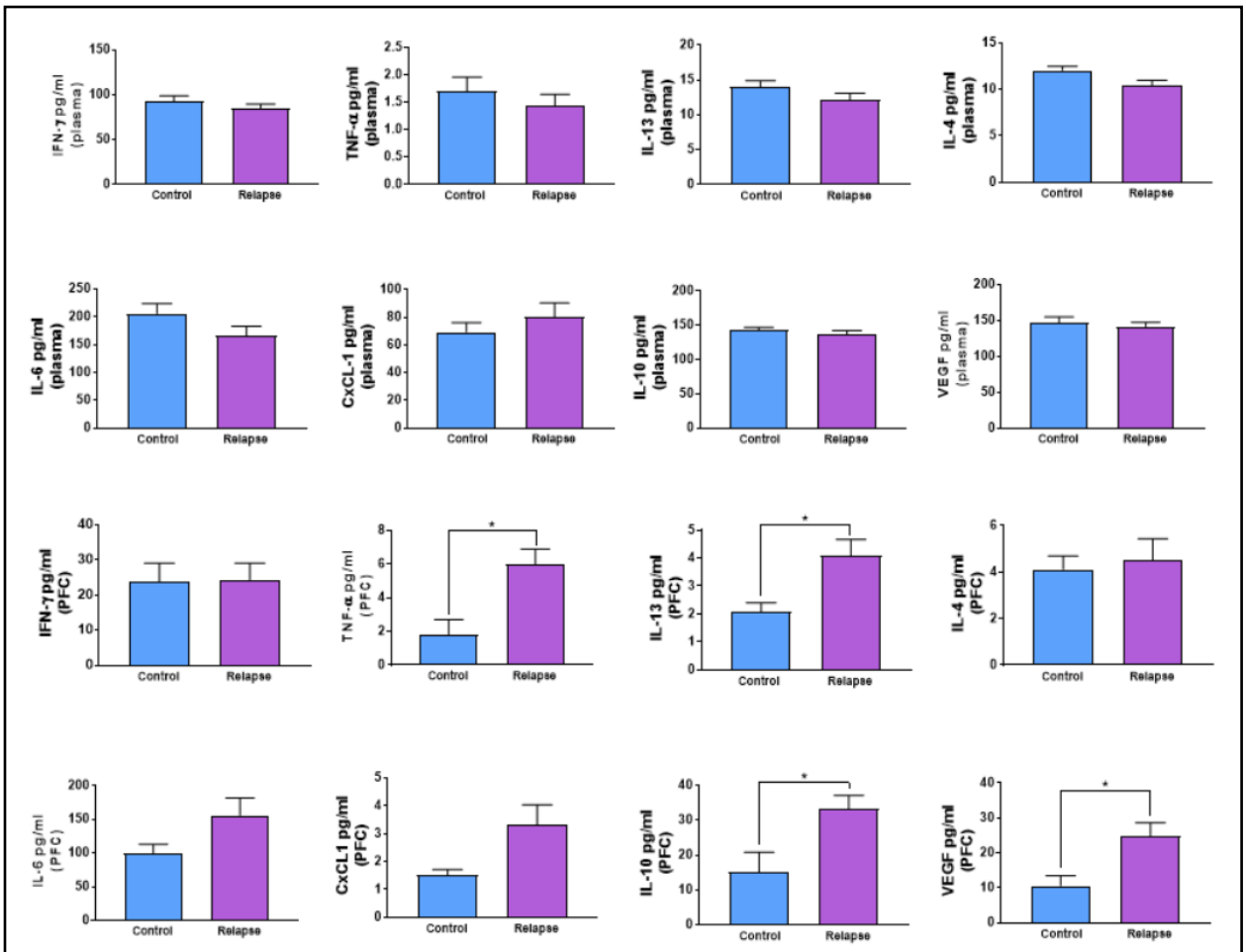

Figure 6: ELISA data analysis of endothelial and neuroimmune markers from plasma and mPFC of alcohol dependent rats after relapse

Cytokines, chemokines, and VEGF were measured in the plasma and mPFC of alcohol dependent rats after relapse. Significant differences were calculated with two-tailed unpaired t-test in TNF-α, IL-13, IL-10, and VEGF expression in the mPFC: *$p \leq 0.05$ between control and relapse. Data are represented as mean ± S.E.M.

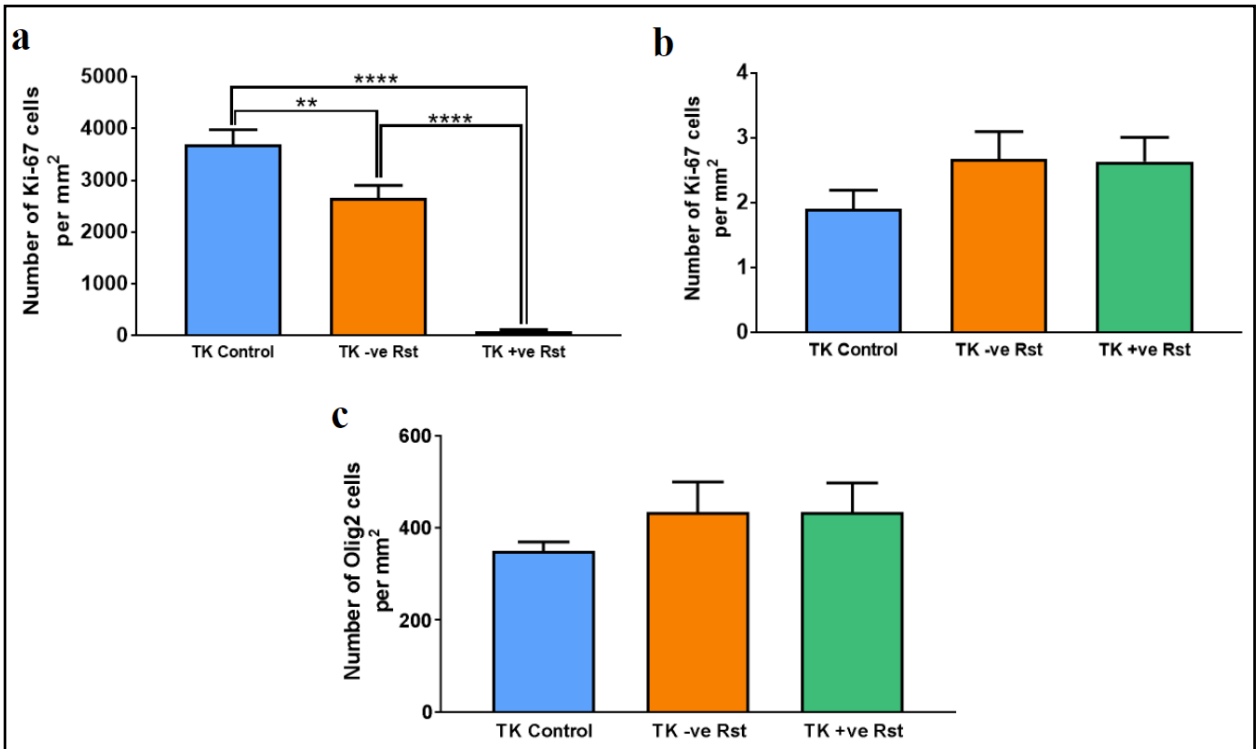

Figure 7: Valcyte treatment effect on Ki-67 expression in the SVZ and mPFC, and Olig2 expression in the mPFC of alcohol dependent rats after reinstatement

Number of cells expressing Ki-67 and Olig2, normalized to cells/mm^2 during reinstatement. One-way ANOVA and post hoc analysis revealed (a) Significant group differences in Ki-67 expression in the SVZ: **$p \leq 0.005$ between control and -ve Rst group; ****$p \leq 0.0001$ between -ve Rst and +ve Rst; ****$p \leq 0.0001$ between control and +ve Rst group. (b) No significant group difference in Ki-67 expression in the mPFC between the three groups, $p \leq 0.05$. (c) No significant group difference in Olig2 expression in the mPFC between the three groups, $p \leq 0.05$. Error bars represent standard error of the mean.

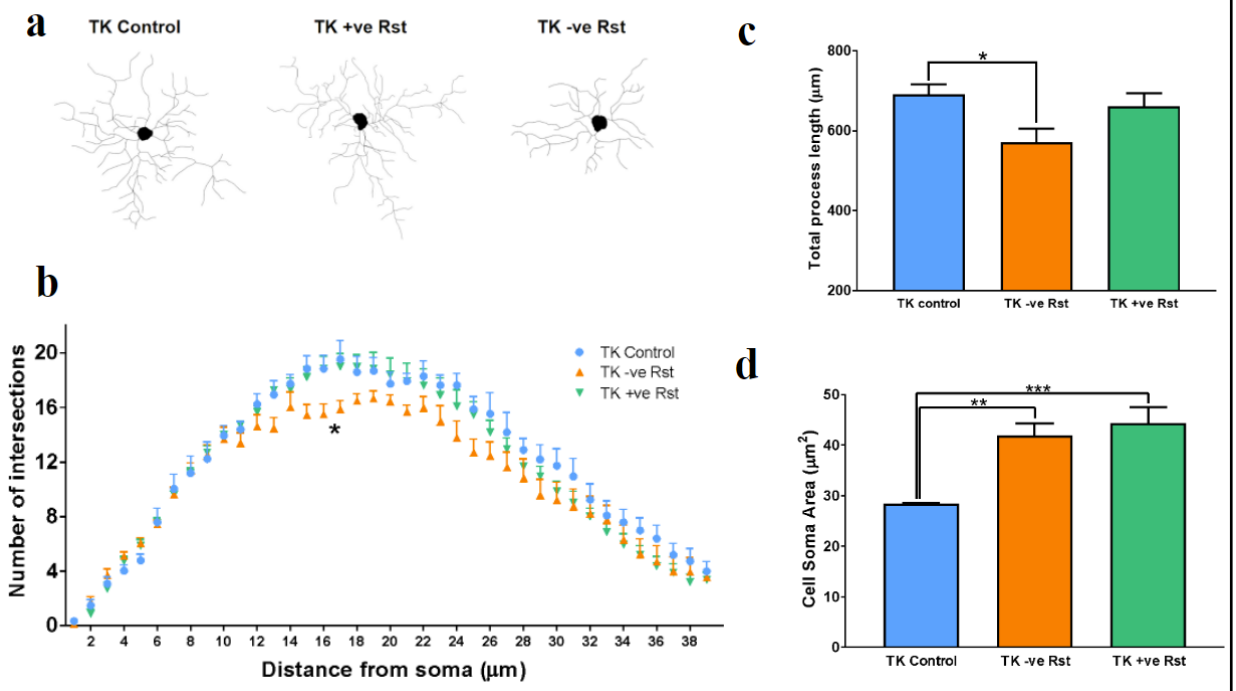

Figure 8: Valcyte treatment effect on microglial morphology in the mPFC of alcohol dependent rats after reinstatement

The mPFC was stained for IBA-1, a marker for microglia. IBA-1 stained microglia were traced using Neurolucida and quantified using Neurolucida Explorer. (**a**) 3D tracing of IBA-1 labeled microglia in the mPFC was done for each group after reinstatement. (**b**) Structural analysis of mPFC microglia is shown as the number of intersections relative to the distance from soma in micrometers. Significant group differences were calculated using two-way ANOVA with multiple comparisons: *p ≤ 0.05 between the control and -ve Rst; *p ≤ 0.05 between the +ve Rst and -ve Rst. Significant group differences were calculated using one-way ANOVA and post hoc analysis: (c) *p ≤ 0.05 between control and -ve Rst group. (d) **p ≤ 0.005 between control and -ve Rst; ***p ≤ 0.0005 between control and +ve Rst. Error bars represent standard error of the mean.

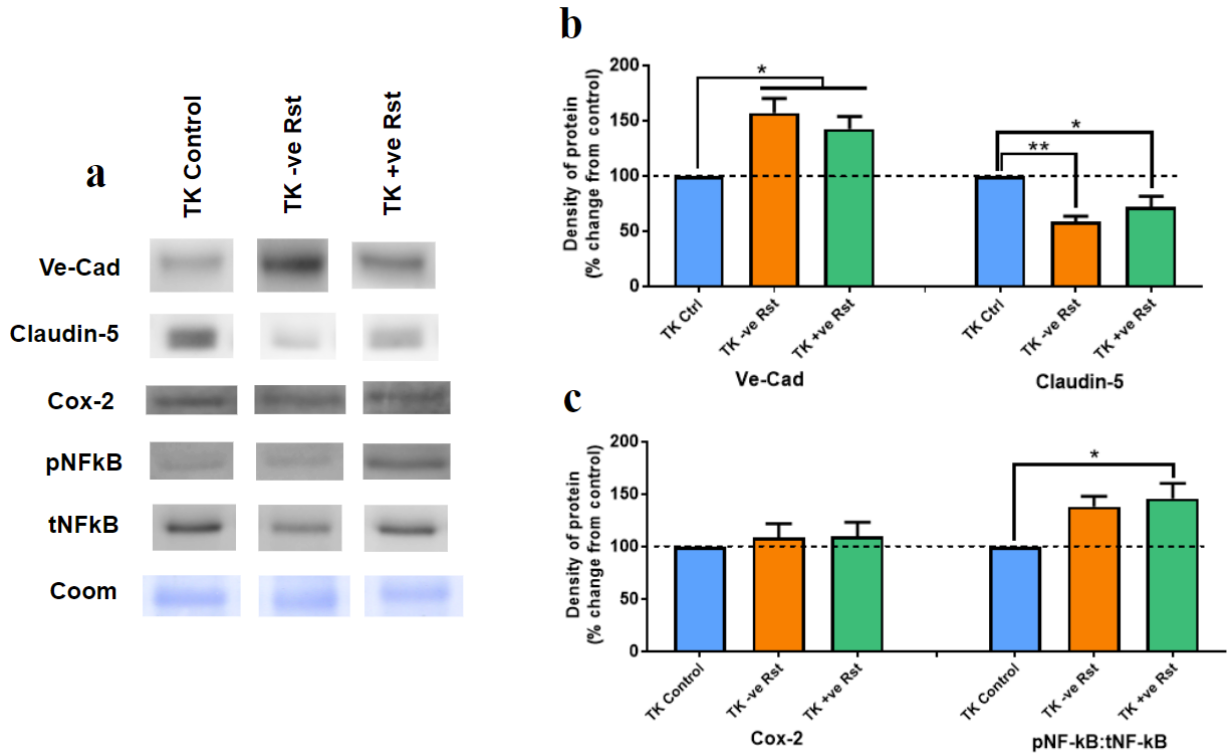

Figure 9: Western blot analysis of endothelial and neuroimmune markers in the mPFC of alcohol dependent rats during reinstatement with Valcyte treatment

Representative immunoblots with corresponding Coomassie (Coom) blot is indicated in (a) Ve-Cadherin (Ve-Cad), Claudin-5, Cox-2, phospo NF-kB (pNF-kB), and total NF-kB (tNF-kB). (b,c) Quantitative data represented as mean ± S.E.M of percent change in density of protein from respective controls (indicated as a dashed line). One-way ANOVA and post hoc analysis: (b) Ve-Cad: *$p \leq 0.05$ between control and -ve Rst, *$p \leq 0.05$ between control and +ve Rst; Claudin-5: **$p \leq 0.005$ between control and -ve Rst, *$p \leq 0.05$ between control and +ve Rst. (c) pNF-kB:tNF-kB: *$p \leq 0.05$ between control and +ve Rst. Error bars represent standard error of the mean.

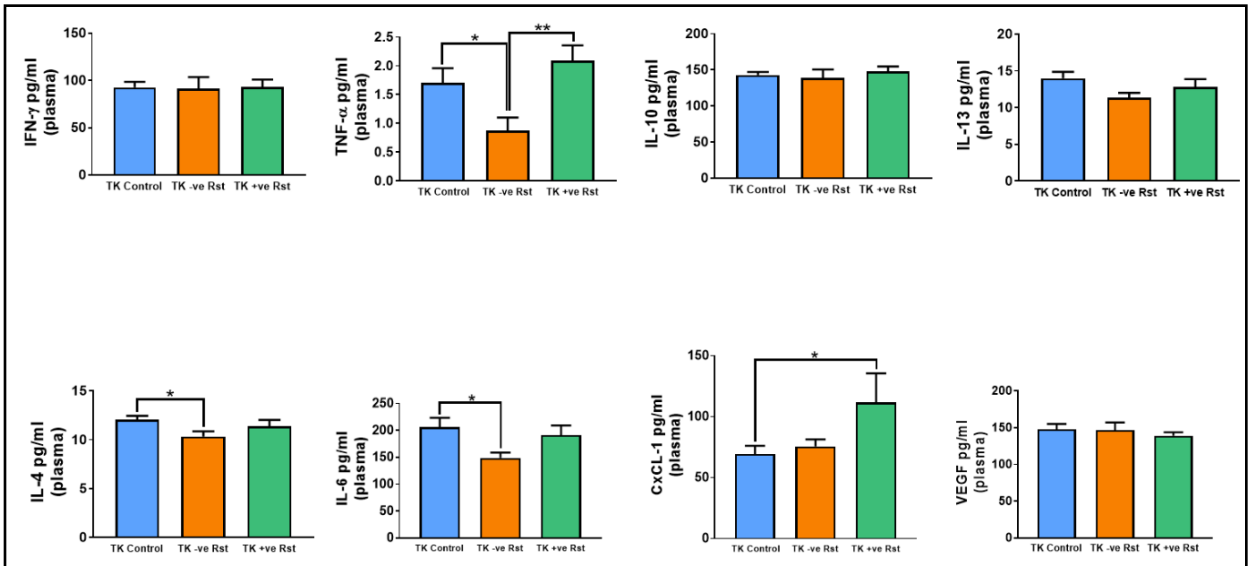

Figure 10: ELISA data analysis of endothelial and immune markers from plasma of alcohol dependent rats after reinstatement with Valcyte treatment

Cytokines, chemokines, and VEGF were measured in the plasma of alcohol dependent rats after reinstatement. Data are represented as mean ± S.E.M. One-way ANOVA and post hoc analysis revealed significant group differences: TNF-α: *$p \leq 0.05$ between control and -ve Rst, **$p \leq 0.005$ between -ve Rst and +ve Rst.; IL-4: *$p \leq 0.05$ between control and -ve Rst.; IL-6: *$p \leq 0.05$ between control and -ve Rst.; CXCL-1: *$p \leq 0.05$ between control and +ve Rst.

RESULTS

CIE enhanced ethanol intake during maintenance (Figure 2a)

Through CIE maintenance, two-way ANOVA revealed a main effect of time ($F_{2,50}$ = 12.89, $p < 0.0001$) without an interaction or main effect of Valcyte. Multiple comparisons revealed a significant increase in ethanol intake between pre CIE and post CIE for both CIE vehicle group ($p = 0.0012$) and Valcyte group ($p = 0.0042$).

Valcyte reduced relapse to drinking behavior in dependent rats (Figure 2a)

Following 3 weeks of abstinence, the vehicle group showed a decrease in ethanol intake from post CIE to relapse ($p = 0.0538$), but an overall increase in ethanol intake when comparing pre CIE to relapse ($p = 0.005$). The CIE exposure increased ethanol intake and was sustained through protracted abstinence. But, in the Valcyte group, there was no significant difference in ethanol intake from pre CIE to relapse ($p = 0.1984$) or between post CIE and relapse ($p = 0.0963$).

Valcyte enhanced latency to extinguish lever pressing behavior in dependent rats during extinction (Figure 2b-c)

Following relapse, rats extinguished lever pressing behavior and two-way ANOVA with repeated measures revealed a main effect of Valcyte ($F_{1,15} = 5.593$, $p = 0.0319$) and main effect of days ($F_{5,75} = 26.32$, $p < 0.0001$), without an interaction. Multiple comparisons analysis with uncorrected Fisher's LSD showed a Valcyte treatment effect with a significant decrease in lever pressing in the Valcyte rats compared to the CIE vehicle rats on day 1 ($p = 0.0072$). To determine the latency of extinction, percent change was calculated between lever responses on

day 1 to all other days (days 2-6) and showed a significant difference between the CIE vehicle and Valcyte group ($p = 0.0526$).

Valcyte reduced reinstatement to ethanol seeking in dependent rats (Figure 2d)

Following 6 days of extinction under a different context, the rats were subject to contextual cued reinstatement. A two-tailed paired t-test revealed a significant increase in lever pressing by the vehicle rats from day 6 of extinction to reinstatement ($t_{(9)} = 3.867$; $p = 0.0048$). Interestingly, this effect was abolished in Valcyte treated CIE rats showing no significant difference in lever pressing from day 6 of extinction to reinstatement $t_{(8)} = 2.06$; $p = 0.0784$).

Proliferation of oligodendrocyte progenitor cells (OPCs) was significantly increased during acute withdrawal in dependent rats; this effect was not sustained through protracted abstinence and relapse (Figure 3a-b)

Newly born progenitor cells were labeled with Ki-67 and data was taken from 3 days post CIE (acute withdrawal) and 21 days post CIE (protracted abstinence and relapse). One-way ANOVA indicated a significant effect in treatment ($F_{2,17} = 15.37$; $p = 0.0002$). Post hoc analysis with uncorrected Fisher's LSD revealed higher Ki-67 expression 3 days post CIE compared to the control group ($p = 0.0002$). In addition, analysis showed lower Ki-67 expression from 3 days post CIE to 21 days post CIE ($p = 0.0001$), but no significant difference between control and relapse group ($p = 0.6312$).

The number of oligodendrocytes were significantly increased after protracted abstinence and relapse in dependent rats (Figure 3c-d)

Oligodendrocytes were labeled with Olig2, and data was taken from 3 days post CIE (acute withdrawal) and 21 days post CIE (protracted abstinence and relapse). One-way ANOVA indicated a significant effect in treatment ($F_{2,17} = 3.592$; $p = 0.05$). Post hoc analysis with uncorrected Fisher's LSD revealed no significant difference in Olig2 expression between control group and 3 days post CIE ($p = 0.5940$) or 3 days post CIE and 21 days post CIE ($p = 0.0673$), but a significant increase in Olig2 expression between the control and relapse group ($p = 0.0261$).

Relapse to drinking altered some aspects of microglial morphology in dependent rats (Figure 4a-c)

Phenotypic analysis of microglia (IBA-1 cells) with two-way ANOVA revealed a main effect of distance from soma ($F_{38,456} = 128.9$; $p < 0.0001$) without an interaction or main effect of group. Multiple comparison analysis revealed no significant difference in the number of intersections at each individual distance (μm) when comparing the control and relapse group. Similarly, two-tailed unpaired t-test showed no significant differences in the total process length between the control and relapse group ($p = 0.7801$). But, when looking at cell soma area (μm^2), there is a significant increase between the control and relapse group ($p = 0.0063$).

Western blot data showed a heightened neuroimmune response in dependent rats after relapse, but did not reveal any changes in BBB integrity (Figure 5a-c)

Western blotting analysis using two-tailed unpaired t-test revealed NF-kB expression was significantly increased in the relapse group compared to the control group ($p = 0.0538$). But no

significant differences in expression were observed in Ve-Cad, Cld-5 and Cox-2 when compared to their respective controls.

ELISA data showed an increase in expression of endothelial and neuroimmune markers in the mPFC of dependent rats after relapse but not in plasma (Figure 6)

Multiplex immunoassays with two-tailed unpaired t-test surprisingly revealed no significant difference between the control and relapse groups in any markers from the plasm data. But in the mPFC, there was a significant increase in expression of TNF-α ($p = 0.0138$), IL-13 ($p = 0.0234$), IL-10 ($p = 0.0393$), and VEGF ($p = 0.0252$) when comparing the relapse to the control group.

Valcyte prevented the generation of progenitor cells in the SVZ, but did not significantly alter the proliferation of OPCs or the number of oligodendrocytes in the mPFC of dependent rats after reinstatement (Figure 7a-c)

One-way ANOVA for Ki-67 cells in the SVZ revealed a significant effect in treatment ($F_{2,18} = 88.46$; $p \leq 0.0001$). Post hoc analysis with uncorrected Fisher's LSD showed a significant decrease in Ki-67 cells between the age matched control and CIE vehicle group ($p = 0.0024$). In the SVZ, Valcyte treatment significantly reduced the number of Ki-67 cells compared to control ($p \leq 0.0001$) and CIE vehicle group ($p \leq 0.0001$). In the mPFC, the number of Ki-67 cells in the CIE groups did not differ from naïve control, and Valcyte did not alter the number of Ki-67 cells ($F_{2,19} = 0.9013$; $p = 0.4227$). Similar to the Ki-67 analysis in the mPFC, the number of Olig2 cells did not differ between the control, vehicle and Valcyte groups ($F_{2,19} = 0.4697$; $p = 0.6323$).

Valcyte prevented some aspects of microglia activation in dependent rats after reinstatement (Figure 8a-d)

Repeated measures two-way ANOVA revealed main effect of distance from soma ($F_{38,684}$ = 152.5; $p \leq 0.0001$) without an interaction or main effect of group. Multiple comparisons analysis with uncorrected Fisher's LSD was performed to compare the number of intersections between the 3 groups at each individual distance (μm). This revealed a decrease in arborization with the control group having a decrease in the number of intersections at distances 15-17, 23-27, 29 μm from soma compared to the vehicle group, $p \leq 0.05$. In addition, a decrease in the number of intersections at distances 13, 15-18, 25 μm from soma comparing vehicle group to the Valcyte group, $p \leq 0.05$. Interestingly, Valcyte increased the number of intersections per distance from soma back to control levels indicated by no significant difference between the control and Valcyte group. Next, analysis of total process length via one-way ANOVA indicated a significant effect in treatment ($F_{2,18}$ = 3.619; p = 0.0477). Post hoc analysis with uncorrected Fisher's LSD revealed a significant decrease in total process length between the control group and vehicle group (p = 0.0258). But Valcyte prevented this decrease in total process length with no significant difference between the control group and the Valcyte group (p = 0.5726). Finally, cell soma area was analyzed by one-way ANOVA showing a significant effect in treatment ($F_{2,19}$ = 8.512; p = 0.0023). Post hoc analysis with uncorrected Fisher's LSD revealed significantly larger cell soma area in the CIE vehicle group compared to the control group (p = 0.003). Valcyte was not able to prevent this increase in cell soma area because there was still a significant increase between the Valcyte and control group (p = 0.0009), with no significant difference between vehicle and Valcyte groups (p = 0.4760).

Western blot analysis showed Valcyte did not prevent endothelial and neuroimmune changes in dependent rats after reinstatement (Figure 9a-c)

One-way ANOVA and post hoc analysis with uncorrected Fisher's LSD was used to analyze all four markers in the mPFC of rats after reinstatement. First, analysis of Ve-Cad revealed a significant effect in treatment ($F_{2,18} = 4.098$; $p = 0.0342$) with a significant increase in Ve-Cad expression between the control group and vehicle group ($p = 0.0105$) and Valcyte group ($p = 0.0515$). Next, Claudin-5 analysis revealed a significant effect in treatment ($F_{2,18} = 5.965$; $p = 0.0103$) with a significant decrease in Claudin-5 expression between the control and vehicle group ($p = 0.0028$) and Valcyte group ($p = 0.0356$). Now looking at neuroimmune markers, no significant effect in treatment was evident for Cox-2 ($F_{2,16} = 0.06654$; $p = 0.9359$). Furthermore, NF-kB did not show a significant effect in treatment ($F_{2,18} = 2.912$; $p = 0.0802$), but multiple comparisons revealed a significant increase between the control group and Valcyte group ($p = 0.0301$).

Valcyte prevented immune response changes in the plasma of dependent rats after reinstatement (Figure 10)

One-way ANOVA and post hoc analysis with uncorrected Fisher's LSD was used to analyze all markers in the plasma of rats after reinstatement. TNF-α analysis indicated a significant effect in treatment ($F_{2,22} = 4.875$; $p = 0.0177$) with a significant decrease in expression between the control group and vehicle group ($p = 0.0314$). Valcyte was able to bring TNF-α expression back to control levels with a significant increase in TNF-α expression between the CIE vehicle and Valcyte group ($p = 0.0061$) and no significant difference between the control and Valcyte group ($p = 0.3041$). Next, IL-4 showed no significant effect in treatment ($F_{2,23} =$

2.689; p = 0.0892), but multiple comparisons revealed a significant decrease in IL-4 expression between the control and vehicle group (p = 0.0296). Valcyte protected against this decrease by having IL-4 levels similar to the control group (p = 0.3634). Furthermore, IL-6 had a significant effect in treatment ($F_{2,22}$ = 3.455; p = 0.0496) with a significant decrease in IL-6 expression between the control and CIE vehicle group (p = 0.0172), but no significant difference between the control and Valcyte group (p= 0.5319). Surprisingly, when looking at CXCL-1, there was no significant effect in treatment ($F_{2,23}$ = 2.67; p = 0.0906), but multiple comparisons revealed a significant increase in CXCL-1 expression between the control group and Valcyte group (p = 0.0365).

DISCUSSION

Our first intention was to investigate ethanol seeking behavior and neurobiological changes in the mPFC of alcohol dependent female rats through protracted abstinence and relapse. First, we wanted to confirm CIE induced alcohol dependency by looking at their ethanol intake (g/kg) levels. Rodents from pre CIE to post CIE had significantly increased and sustained their ethanol intake through relapse, indicating CIE successfully produced alcohol dependency that mimicked moderate to severe AUD.

Previous studies have shown a proliferative burst of OPCs in the mPFC of male dependent rats 3 days into abstinence that has been linked to heightened anxiety and stress (Somkuwar *et al.*, 2016a, b; Somkuwar *et al.*, 2017b). To see if this proliferative burst was present in females as well, we did immunohistochemistry analysis for Ki-67 cells in the mPFC. The results showed a significant increase in Ki-67 cells when comparing the control and alcohol dependent rats 3 days into abstinence, indicating the presence of a proliferative burst of OPCs. Interestingly, this burst was not sustained through protracted abstinence with a significant decrease in Ki-67 cells from 3 days post CIE to 21 days post CIE. These results suggest that the rebound effect in Ki-67 cells is transient and could contribute to enhanced generation of oligodendrocytes during protracted abstinence. To investigate alterations in the number of oligodendrocytes, we quantified the number of Olig2 cells. Somkuwar *et al.* (2016b) showed that the burst of OPCs survive and differentiate into myelinating oligodendrocytes in the mPFC of male dependent rats after protracted abstinence. Our data mirrors this in female rats by showing a significant increase in Olig2 cells between the control and 21 days post CIE group. In summary, a proliferative burst of OPCs is prominent in the mPFC during acute withdrawal revealing OPCs probably mature into oligodendrocytes in protracted abstinence. Additional co-labeling analysis

will confirm these findings. Taken together, the increases in Olig2 cells could be indicative of the repair of brain tissue during abstinence or increases in immune responses in the brain as seen in conditions such as ischemic stroke (Ohab & Carmichael, 2008; Arai & Lo, 2009).

Since ethanol dependence has been associated with significant neuroimmune responses (Crews, 2012), a neuroimmune factor that was analyzed was microglia morphology in the mPFC of alcohol dependent rats after protracted abstinence and relapse. When comparing the control and CIE relapse group, we saw no significant difference in the number of intersections per distance from soma or total dendritic length, indicating there was no change in microglial state due to chronic alcohol exposure and protracted abstinence. But the cell soma area, another aspect of microglial morphology, was significantly increase in the relapse group compared to the control group. This data suggests there was a neuroimmune response in rodents that demonstrated relapse to ethanol drinking and altered one certain aspect of microglia morphology. After seeing this change, Western blot analysis was performed to investigate other neuroimmune markers and endothelial changes in rats that relapsed.

The endothelial and immune markers analyzed were Ve-Cadherin, Claudin-5, Cox-2, and NF-kB. Ve-Cadherin is an adherens junction protein that stabilizes cell to cell adhesion via actin filaments and keeps endothelial tissues from separating, thus regulates vascular permeability (Li *et al.*, 2018; Gavard & Gutkind, 2008). Claudin-5 is a tight junction protein that maintains structural integrity of vasculature and regulates movement of molecules in and out of the cell (Greene *et al.*, 2019). Previous studies have suggested Ve-Cadherin controls Claudin-5 expression, and both change in response to neuroinflammation causing BBB disruption (Gavard & Gutkind, 2008; Li *et al.*, 2018). Surprisingly, our data shows no significant difference in Ve-Cadherin and Claudin-5 levels indicating no endothelial changes or BBB disruption present in

dependent rats during relapse. For Western blot analysis we also look at Cox-2 and NF-kB which are pro-inflammatory mediators and when oxidative stress or an environmental threat is present, they become upregulated to induce inflammatory cascades (Liu *et al.*, 2017; Rawat *et al.*, 2019). Previous studies have shown enhanced NF-kB expression in CIE-ED female rats in the mPFC which has been implicated in AUD individuals as well (Avchalumov *et al*., 2021). Our data indicated no significant change in expression of Cox-2 between the control and relapse group in the mPFC. However, there was a significant increase in NF-kB expression depicting a heightened neuroimmune response during relapse in dependent female rats. NF-kB is known to play a significant role in inflammation by inducing the production of multiple cytokines, so we chose to look at different cytokines via multiplex immunoassays (Liu *et al.*, 2017).

Multiplex immunoassays looked for multiple cytokines and an endothelial marker in the plasma and brain of alcohol dependent rats. Since alcohol has a systemic effect on the body, we chose to analyze plasma in addition to the brain. Surprisingly, there were no significant differences in expression of any markers in the plasma when comparing the control and relapse groups. In contrast, analysis of the mPFC showed a significant increase in TNF-α, IL-13, IL-10, and VEGF expression. An increase in TNF-α production is induced by enhanced NF-kB signaling that promotes production of pro-inflammatory cytokines, which is prominent in our data as well (Liu *et al.*, 2017). TNF-α is an important inflammatory cytokine that leads to vasodilation contributing to oxidative stress and apoptosis in sites of inflammation (Idriss *et al.*, 2000). IL-13 and IL-10 can have both pro- and anti-inflammatory properties, but the prominent increase evident could be the brain combating or responding to this alcoholic immune challenge by increasing these anti-inflammatory cytokines. In addition, there was an increase in VEGF expression in the mPFC of the dependent relapse group. VEGF is important in angiogenesis to

stimulate the formation of blood vessels and increasing endothelial proliferation. It has been implicated as a pro-inflammatory response via NF-kB signaling leading to BBB permeability (Kim *et al.*, 2001; Reinders *et al.*, 2003; Yano *et al.*, 2006). An increase in VEGF is a marker for a heightened neuroimmune response and endothelial damage that needs repair (Li *et al.*, 2018). Overall, this data showed the ability of ethanol to pass the BBB, create an increased neuroimmune response and endothelial changes in the brain; but did not have a significant systemic effect in alcohol dependent rats after relapse. Thus, we do not see a correlation between plasma and brain changes due to chronic ethanol exposure in female dependent rats.

Given that we found significant changes in behavior, neuroimmune responses and BBB dysfunction were prominent after relapse to ethanol seeking, our second goal was to investigate the role the burst of proliferating cells seen in early withdrawal has on reinstatement to ethanol seeking behaviors and neurobiological responses seen in dependent rats. To prevent this proliferative burst, transgenic rats expressing HSV-TK under the GFAP promoter were given Valcyte.

First, we wanted to compare ethanol intake between rats that were designated Valcyte and CIE vehicle groups through relapse. Since Valcyte treatment only began during the last week of maintenance, it was important to observe similar ethanol drinking behavior and consumption between the two groups. Both groups significantly increase their ethanol intake due to CIE, indicating alcohol dependency. Since Valcyte treatment was continued during abstinence, the next question was to determine if Valcyte affected drinking during relapse. Interestingly, Valcyte reduced alcohol drinking during relapse with no significant increase in ethanol intake between the pre CIE and relapse group. Thus, Valcyte decreased relapse to ethanol seeking in alcohol dependent rats. Next, lever pressing behavior during day 1 of extinction showed the Valcyte

group lever pressed significantly less than the CIE vehicle group indicating reduced motivation for ethanol seeking. This reduced motivation was emphasized when looking at nonlinear regression analysis for latency to extinguish with the Valcyte group having faster latency to extinguish compared to the vehicle group. Thus, preventing the burst of progenitor cells helped that rats extinguish faster, learn new behavior quicker and showed less motivation to drink. Finally, comparing lever pressing from day 6 of extinction to reinstatement, the vehicle treated ethanol dependent rats lever pressed significantly more during reinstatement when compared with Valcyte treated females. This data indicated that Valcyte prevented alcohol dependent rats from reinstating lever pressing behavior and decreased motivational alcohol seeking. Taken together these behavioral data sets showed that Valcyte not only protected rats against ethanol seeking during relapse but also reduced motivation to lever pressing and ethanol seeking behavior during reinstatement. Next, analysis of neural cells was done to see if Valcyte treatment prevented the generation of progenitor cells.

Since Valcyte targets progenitors of GFAP origin (Snyder *et al.*, 2016), and that the subventricular zone (SVZ) is populated with progenitors of GFAP origin unlike the mPFC (where the progenitors are of NG2 glial origin; Somkuwar *et al*., 2014), we performed Ki-67 analysis in the SVZ to confirm Valcyte effect on progenitor apoptosis. Our data showed a significant decrease in Ki-67 cells in the SVZ with Valcyte compared to the vehicle group indicating the drug was effective in ablating progenitor cells in the SVZ. In addition, our data showed that SVZ cells were also affected by alcohol dependence and that the number of cells were reduced in rats that had reinstated ethanol seeking behavior. Previous work has demonstrated that proliferating cells from the SVZ migrate to the PFC and other cortical areas under conditions such as stroke and ischemia (Somkuwar *et al*., 2014), and we hypothesized that

this type of migration of cells from SVZ to PFC could be occurring during acute withdrawal from ethanol dependence. Therefore, Valcyte treatment would only block progenitors that were sensitive to its treatment and could prevent any migration of cells from the SVZ to PFC during acute withdrawal. In this context, Ki-67 analysis in the mPFC after reinstatement showed no significant difference between the Valcyte and vehicle groups suggesting that the cells present in the PFC were not Valcyte sensitive, and not from GFAP origin. This data suggests that Valcyte could have prevented the migration of cells from SVZ to mPFC during acute withdrawal, or that abstinence following withdrawal could have ablated the cells in the mPFC that were from GFAP origin. These issues need to be investigated. In addition, we did not see a significant difference in oligodendrocytes between the control and vehicle group that had reinstated ethanol seeking, meaning the Ki-67 burst did not result in an increased number of Olig2 cells after protracted abstinence and reinstatement. Furthermore, there was no significant difference in the number of Olig2 cells between the vehicle and Valcyte group, indicating that Valcyte treatment did not alter Olig2 cells in the PFC and suggesting that Olig2 cells may be generated by cells from non GFAP origin. Because Valcyte protected dependent rats from relapse and reinstatement and successfully abolished the proliferative burst, we wanted to see the effect of Valcyte treatment on other neuroimmune responses after reinstatement.

Previous research has shown microglia in the mPFC of CIE rats have activated microglia morphology with simplified branching compared to controls and a decrease in the number of intersections per distance from soma, indicating a heightened immune response due to chronic alcohol exposure (Avchalumov *et al.*, 2021; Siemsen *et al.*, 2021). Our study aligns with these previous findings by showing a significant decrease in the number of intersections per distance from soma when comparing the vehicle to the control group, indicating chronic alcohol exposure

and reinstatement caused activation of microglia. Interestingly, a novel finding from our experiment showed that when Valcyte treatment was given there was no significant difference in the number of intersections relative to distance from soma compared to the control or CIE vehicle group. Thus, Valcyte prevented the change in arborization and this aspect of microglial activation. In addition, total process length mirrored the arborization data with a significant decrease in total process length in the CIE vehicle compared to the control group indicating microglia activation, but Valcyte prevented this decrease and brought processes length back to control levels. Finally, microglia cell soma area was investigated to illustrate a significant increase in soma area between the control and both reinstatement groups indicating an activated microglial state. Valcyte treatment did not change cell soma area microglia morphology in alcohol dependent rats through reinstatement. This data suggests that Valcyte was able to prevent certain morphological alterations in microglial cells and this could correlate with normalizing other neuroimmune markers or markers of BBB dysfunction.

Neuroinflammation can result in BBB dysfunction by disrupting adherens junctions and tight junctions (Li *et al.*, 2018). This was specifically evident in alcohol dependent female rats with a significant decrease in Claudin-5 levels in the mPFC (Avchalumov *et al.*, 2021). In addition, ischemic stroke patients show increased amounts of Ve-Cadherin in endothelial cells indicating BBB dysregulation associated with neuroinflammation (Li *et al.*, 2018). Our Western blotting data supports previous studies by with an increase in Ve-Cadherin expression and decrease in Claudin-5 levels between the control and CIE vehicle group indicating prominent endothelial damage and decrease in BBB integrity during reinstatement. In addition, a significant difference was still prominent between the control and Valcyte group in Ve-Cadherin and Claudin-5 levels indicating Valcyte did not protect against this aspect of endothelial change.

When analyzing neuroimmune markers, Cox-2 levels were not influenced by protracted abstinence and reinstatement in alcohol dependent female rats. But NF-kB expression was significantly increased between the control and Valcyte group. Overall, the Western blot data illustrated certain neuroimmune adaptations that are present after relapse persist into reinstatement and Valcyte did not alter these specific markers. While there were no significant changes between the vehicle and Valcyte groups, we still support a neuroimmune activated state and BBB disruption in alcohol dependent rats through reinstatement. Since endothelial damage and an inflammatory response was prominent, further analysis was done on the expression of cytokines, chemokines, and VEGF with Valcyte treatment.

Multiplex immunoassays now focused on plasma data because Valcyte was given orally, and we wanted to see what changes arise in the periphery due to this treatment. Interestingly, the plasma data showed significant changes in levels of TNF-α, IL-4, and IL-6 through reinstatement when there were no changes in these cytokines during relapse. Importantly, Valcyte treatment reversed the decrease in TNF-α, IL-4, and IL-6 levels back to control numbers with no significant difference between the control and Valcyte groups. To our surprise, we see a significant increase in CXCL-1 levels comparing the control and Valcyte group. It is unclear what this change means, but future analysis can be done to compare the plasma changes to the PFC to get more insight on this data. In summary, Valcyte prevented periphery changes caused by chronic alcohol exposure after protracted abstinence and reinstatement.

Overall, our data showed chronic alcohol exposure affected ethanol seeking behavior and caused immune and BBB integrity changes through protracted abstinence and relapse in the mPFC of female rats. In addition, Valcyte was able to protect against ethanol seeking behavior and some of these biological changes seen in the mPFC and plasma of female dependent rats

through reinstatement. In conclusion, stopping the proliferative burst during acute withdrawal decreased ethanol seeking behavior by preventing some aspects of the immune response seen in protracted abstinence.

Future directions that can be explored are obtaining ELISA data from the mPFC of Valcyte and vehicle alcohol dependent female rats after reinstatement. This data will allow us to further understand how Valcyte treatment is changing neuroimmune markers and can also be compared to the plasma data. In addition, data collection was performed 3 days into abstinence, after relapse and reinstatement. In the future, two different timepoints should be analyzed which include right after 7 weeks of CIE maintenance and after 3 weeks of abstinence, but before relapse. This will allow us to determine specificity and causation for neuroimmune and endothelial changes that are present through the different timepoints in this experimental design. For example, we saw an increase in cell soma area that was sustained through relapse and reinstatement but could not pinpoint when this increase specifically started or what caused it. From our current data it is unclear if the increase in soma area was solely due to CIE maintenance, abstinence, or relapse. Furthermore, in my research we show data in the prefrontal cortex, but another important brain region to consider is the hippocampus. The hippocampus is where these GFAP progenitor cells are born and a target of Valcyte. Further analysis would involve looking at how Valcyte affects oligodendrogenesis, endothelial and neuroimmune changes in the hippocampus differentially than the mPFC. Also, my research focused solely on females, but our lab is currently performing this entire experiment on males. In the future we will be able to compare female and male dependent rats to see if there is a sex differentiation in the neurobiological response to Valcyte treatment.

REFERENCES

Arai, K., & Lo, E. H. (2009). Experimental models for analysis of oligodendrocyte pathophysiology in stroke. *Experimental & translational stroke medicine*, *1*, 6. https://doi.org/10.1186/2040-7378-1-6

Avchalumov, Y., Kreisler, A. D., Xing, N., Shayan, A. A., Bharadwaj, T., Watson, J. R., Sibley, B., Somkuwar, S. S., Trenet, W., Olia, S., Piña-Crespo, J. C., Roberto, M., & Mandyam, C. D. (2021). Sexually dimorphic prelimbic cortex mechanisms play a role in alcohol dependence: protection by endostatin. *Neuropsychopharmacology*, *46*(11), 1937–1949. https://doi.org/10.1038/s41386-021-01075-6

Avegno, E. M., & Gilpin, N. W. (2019). Inducing Alcohol Dependence in Rats Using Chronic Intermittent Exposure to Alcohol Vapor. *Bio-protocol*, *9*(9), e3222. https://doi.org/10.21769/BioProtoc.3222

Becker, J. B., & Koob, G. F. (2016). Sex differences in animal models: Focus on addiction. In *Pharmacological Reviews* (Vol. 68, Issue 2, pp. 242–263). American Society for Pharmacology and Experimental Therapy. https://doi.org/10.1124/pr.115.011163

Cohen, A., Soleiman, M.T., Talia, R., Koob, G.F., George, O., Mandyam, C.D., (2015). Extended access nicotine self-administration with periodic deprivation increases immature neurons in the hippocampus. Psychopharmacology 232, 453–463.

Courtney, K.E., Polich, J., (2009). Binge drinking in young adults: data, definitions, and determinants. Psychol. Bull. 135, 142–156.

Crews F. T. (2012). Immune function genes, genetics, and the neurobiology of addiction. *Alcohol research: current reviews*, *34*(3), 355–361.

Ernst, A.J., Dempster, J.P., Yee, R., Dennis, C., Nakano, L., (1976). Alcohol toxicity, blood alcohol concentration and body water in young and adult rats. J. Stud. Alcohol 37, 347–356.

Fannon,, M. J., Mysore, K. K., Williams, J., Quach, L. W., Purohit, D. C., Sibley, B. D., Sage Sepulveda, J. S., Kharidia, K. M., Morales Silva, R. J., Terranova, M. J., Somkuwar, S. S., Staples, M. C., & Mandyam, C. D. (2018). Hippocampal neural progenitor cells play a distinct role in fear memory retrieval in male and female CIE rats. *Neuropharmacology*, *143*, 239–249. https://doi.org/10.1016/j.neuropharm.2018.09.045

Fowler, A.-K., Thompson, J., Chen, L., Dagda, M., Dertien, J., Dossou, K. S. S., Moaddel, R., Bergeson, S. E., & Kruman, I. I. (2014). Differential Sensitivity of Prefrontal Cortex and Hippocampus to Alcohol-Induced Toxicity. *PLoS ONE*, *9*(9), e106945. https://doi.org/10.1371/journal.pone.0106945

Galinato, M.H., Orio, L., Mandyam, C.D., (2015). Methamphetamine differentially affects BDNF and cell death factors in anatomically defined regions of the hippocampus. Neuroscience 286, 97–108.

Gavard, J., & Gutkind, J. S. (2008). VE-cadherin and claudin-5: it takes two to tango. *Nature Cell Biology*, *10*(8), 883–885. https://doi.org/10.1038/ncb0808-883

Gilpin, N. W., Richardson, H. N., Cole, M., & Koob, G. F. (2008). Vapor inhalation of alcohol in rats. Current protocols in neuroscience, Chapter 9, Unit–9.29.

Greene, C., Hanley, N., & Campbell, M. (2019). Claudin-5: gatekeeper of neurological function. *Fluids and Barriers of the CNS*, *16*(1), 3. https://doi.org/10.1186/s12987-019-0123-z

Idriss, H. T., & Naismith, J. H. (2000). TNF alpha and the TNF receptor superfamily: structure-function relationship(s). *Microscopy research and technique*, *50*(3), 184–195. https://doi.org/10.1002/1097-0029(20000801)50:3<184::AID-JEMT2>3.0.CO;2-H

Kim, I., Moon, S.O., Kim, S.H., Kim, H.J., Koh, Y.S. & Koh, G.Y. (2001) Vascular endothelial growth factor expression of intercellular adhesion molecule 1 (ICAM-1), vascular cell adhesion molecule 1 (VCAM-1), and E-selectin through nuclear factor-kappa B activation in endothelial cells. *J Biol Chem*, 276, 7614-7620.

Kim, A., Zamora-Martinez, E. R., Edwards, S., & Mandyam, C. D. (2014). Structural reorganization of pyramidal neurons in the medial prefrontal cortex of alcohol dependent rats is associated with altered glial plasticity. Brain Structure and Function, 220(3), 1705–1720. doi: 10.1007/s00429- 014-0755-3

Koob, G. F., & Volkow, N. D. (2010). Neurocircuitry of addiction. *Neuropsychopharmacology: official publication of the American College of Neuropsychopharmacology*, *35*(1), 217–238. https://doi.org/10.1038/npp.2009.110

Kranzler, H. R., & Soyka, M. (2018). Diagnosis and Pharmacotherapy of Alcohol Use Disorder: A Review. *JAMA*, *320*(8), 815–824. https://doi.org/10.1001/jama.2018.11406

Li, W., Chen, Z., Chin, I., Chen, Z., & Dai, H. (2018). The Role of VE-cadherin in Blood-brain Barrier Integrity Under Central Nervous System Pathological Conditions. *Current neuropharmacology*, *16*(9), 1375–1384. https://doi.org/10.2174/1570159X16666180222164809

Liu, T., Zhang, L., Joo, D., & Sun, S.-C. (2017). NF-κB signaling in inflammation. *Signal Transduction and Targeted Therapy*, *2*(1), 17023. https://doi.org/10.1038/sigtrans.2017.23

Mandyam, C.D., Norris, R.D., Eisch, A.J., 2004. Chronic morphine induces premature mitosis of proliferating cells in the adult mouse subgranular zone. J. Neurosci. Res. 76, 783–794.

Mandyam, C. D., Villalpando, E. G., Steiner, N.L., Quach, L.W., Fannon, M.J., Somkuwar, S.S. (2017) Platelet Endothelial Cell Adhesion Molecule-1 and Oligodendrogenesis: Significance in Alcohol Use Disorders. *Brain Sciences,* 7(131). http://doi.org/10.3390/brainsci7100131. Review.

Navarro, A.I., Mandyam, C.D. (2015). Protracted abstinence from chronic ethanol exposure alters the structure of neurons and expression of oligodendrocytes and myelin in the medial prefrontal cortex. Neuroscience. 293:35–44.

O'Dell, L. E., Roberts, A. J., Smith, R. T., & Koob, G. F. (2004). Enhanced alcohol self administration after intermittent versus continuous alcohol vapor exposure. *Alcoholism, clinical and experimental research*, *28*(11), 1676–1682. https://doi.org/10.1097/01.alc.0000145781.11923.4e

Ohab, J. J., & Carmichael, S. T. (2008). Poststroke neurogenesis: emerging principles of migration and localization of immature neurons. *The Neuroscientist: a review journal bringing neurobiology, neurology and psychiatry*, *14*(4), 369–380. https://doi.org/10.1177/1073858407309545

Paxinos, G., Watson, C., (1997). The Rat Brain in Stereotaxic Coordinates. Academic Press, San Diego.

Randall, P. A., Stewart, R. T., & Besheer, J. (2017). Sex differences in alcohol self-administration and relapse-like behavior in Long-Evans rats. *Pharmacology Biochemistry and Behavior*, *156*. https://doi.org/10.1016/j.pbb.2017.03.005

Rawat, C., Kukal, S., Dahiya, U. R., & Kukreti, R. (2019). Cyclooxygenase-2 (COX-2) inhibitors: future therapeutic strategies for epilepsy management. *Journal of Neuroinflammation*, *16*(1), 197. https://doi.org/10.1186/s12974-019-1592-3

Reinders, M.E., Sho, M., Izawa, A., Wang, P., Mukhopadhyay, D., Koss, K.E., Geehan, C.S., Luster, A.D., Sayegh, M.H. & Briscoe, D.M. (2003) Proinflammatory functions of vascular endothelial growth factor in alloimmunity. *J Clin Invest*, 112, 1655-1665.

Siemsen, B. M., Landin, J. D., McFaddin, J. A., Hooker, K. N., Chandler, L. J., & Scofield, M. D. (2021). Chronic intermittent ethanol and lipopolysaccharide exposure differentially alter Iba1-derived microglia morphology in the prelimbic cortex and nucleus accumbens core of male Long-Evans rats. *Journal of neuroscience research*, *99*(8), 1922–1939. https://doi.org/10.1002/jnr.24683

Snyder, J. S., Grigereit, L., Russo, A., Seib, D. R., Brewer, M., Pickel, J., & Cameron, H. A. (2016). A Transgenic Rat for Specifically Inhibiting Adult Neurogenesis. *eNeuro*, *3*(3), ENEURO.0064-16.2016. https://doi.org/10.1523/ENEURO.0064-16.2016

Somkuwar, S.S., Fannon-Pavlich, M.J., Ghofranian, A., Quigley, J. A., Dutta, R. R., Galinato, M. H., & Mandyam, C. D. (2016a). Wheel running reduces ethanol seeking by increasing neuronal activation and reducing oligodendroglial/neuroinflammatory factors in the medial prefrontal cortex. *Brain, behavior, and immunity*, *58*, 357–368. https://doi.org/10.1016/j.bbi.2016.08.006

Somkuwar, S.S., Fannon-Pavlich, M.J., Nguyen, B.T, Mandyam, C.D. (2017a) Hyper oligodendrogenesis at the vascular niche and reduced blood-brain barrier integrity in the

prefrontal cortex during protracted abstinence. *Neuroscience*, *362*, 265-271. https://doi.org/10.1016/j.neuroscience.2017.08.048

Somkuwar, S.S., Fannon-Pavlich, M.J., Staples, M.C., Zamora-Martinez, E.R., Navarro, A.I., Kim, A., Quigley, J.A., Edwards, S., & Mandyam, C.D. (2016b). Alcohol dependence-induced regulation of the proliferation and survival of adult brain progenitors is associated with altered BDNF-TrkB signaling. *Brain structure & function*, *221*(9), 4319–4335. https://doi.org/10.1007/s00429-015-1163-z

Somkuwar, S. S., Staples, M. C., Galinato, M. H., Fannon, M. J., & Mandyam, C. D. (2014). Role of NG2 expressing cells in addiction: a new approach for an old problem. *Frontiers in pharmacology*, *5*, 279. https://doi.org/10.3389/fphar.2014.00279

Somkuwar, S. S., Vendruscolo, L. F., Fannon, M. J., Schmeichel, B. E., Nguyen, T. B., Guevara, J., Sidhu, H., Contet, C., Zorrilla, E. P., & Mandyam, C. D. (2017b). Abstinence from prolonged ethanol exposure affects plasma corticosterone, glucocorticoid receptor signaling and stress-related behaviors. *Psychoneuroendocrinology*, *84*, 17–31. https://doi.org/10.1016/j.psyneuen.2017.06.006

Somkuwar, S. S., Villalpando, E. G., Quach, L. W., Head, B. P., McKenna, B. S., Scadeng, M., & Mandyam, C. D. (2021). Abstinence from ethanol dependence produces concomitant cortical gray matter abnormalities, microstructural deficits and cognitive dysfunction. *European neuropsychopharmacology: the journal of the European College of Neuropsychopharmacology*, *42*, 22–34. https://doi.org/10.1016/j.euroneuro.2020.11.010

Staples, M.C., Somkuwar, S.S., Mandyam, C.D., 2015. Developmental effects of wheel running on hippocampal glutamate receptor expression in young and mature adult rats. Neuroscience 305, 248–256.

Takashima, Y., Fannon, M. K. J., Galinato, M. H., Steiner, N. L., An, M., Zemljic-Harpf, A. E., Somkuwar, S. S., Head, B. P., & Mandyam, C. D. (2018). Neuroadaptations in the dentate gyrus following contextual cued reinstatement of methamphetamine seeking. *Brain Structure and Function*, *223*(5), 2197–2211. https://doi.org/10.1007/s00429-018-1615-3

Thacker, J. S., Yeung, D. H., Staines, W. R., & Mielke, J. G. (2016). Total protein or high-abundance protein: Which offers the best loading control for Western blotting?. *Analytical biochemistry*, *496*, 76–78. https://doi.org/10.1016/j.ab.2015.11.022

Torres, O. v., Walker, E. M., Beas, B. S., & O'Dell, L. E. (2014). Female Rats Display Enhanced Rewarding Effects of Ethanol That Are Hormone Dependent. *Alcoholism: Clinical and Experimental Research*, *38*(1). https://doi.org/10.1111/acer.12213

Wang, Y. L., Han, Q. Q., Gong, W. Q., Pan, D. H., Wang, L. Z., Hu, W., Yang, M., Li, B., Yu, J., & Liu, Q. (2018). Microglial activation mediates chronic mild stress-induced depressive- and anxiety-like behavior in adult rats. Journal of Neuroinflammation, 15(1). https://doi.org/10.1186/s12974-018-1054-3

Warden, A. S., Wolfe, S. A., Khom, S., Varodayan, F. P., Patel, R. R., Steinman, M. Q., Bajo, M., Montgomery, S. E., Vlkolinsky, R., Nadav, T., Polis, I., Roberts, A. J., Mayfield, R. D., Harris, R. A., & Roberto, M. (2020). Microglia Control Escalation of Drinking in Alcohol-Dependent Mice: Genomic and Synaptic Drivers. *Biological psychiatry*, *88*(12), 910–921. https://doi.org/10.1016/j.biopsych.2020.05.011

Welinder, C., & Ekblad, L. (2011). Coomassie staining as loading control in Western blot analysis. *Journal of proteome research*, *10*(3), 1416–1419. https://doi.org/10.1021/pr1011476

Yano, K., Liaw, P.C., Mullington, J.M., Shih, S.C., Okada, H., Bodyak, N., Kang, P.M., Toltl, L., Belikoff, B., Buras, J., Simms, B.T., Mizgerd, J.P., Carmeliet, P., Karumanchi, S.A. & Aird, W.C. (2006) Vascular endothelial growth factor is an important determinant of sepsis morbidity and mortality. *J Exp Med*, 203, 1447-1458.